

# UC Irvine

## UC Irvine Previously Published Works

### Title

Constraints on Asian and European sources of methane from CH<sub>4</sub>-C<sub>2</sub>H<sub>6</sub>-CO correlations in Asian outflow

### Permalink

<https://escholarship.org/uc/item/7xz0029k>

### Journal

Journal of Geophysical Research, 109(D15)

### ISSN

0148-0227

### Authors

Xiao, Yaping  
Jacob, Daniel J  
Wang, James S  
[et al.](#)

### Publication Date

2004

### DOI

10.1029/2003jd004475

### Copyright Information

This work is made available under the terms of a Creative Commons Attribution License, available at <https://creativecommons.org/licenses/by/4.0/>

Peer reviewed

## Constraints on Asian and European sources of methane from CH<sub>4</sub>-C<sub>2</sub>H<sub>6</sub>-CO correlations in Asian outflow

Yaping Xiao,<sup>1</sup> Daniel J. Jacob,<sup>1</sup> James S. Wang,<sup>1,2</sup> Jennifer A. Logan,<sup>1</sup> Paul I. Palmer,<sup>1</sup> Parvatha Suntharalingam,<sup>1</sup> Robert M. Yantosca,<sup>1</sup> Glen W. Sachse,<sup>3</sup> Donald R. Blake,<sup>4</sup> and David G. Streets<sup>5</sup>

Received 21 December 2003; revised 16 April 2004; accepted 14 May 2004; published 10 August 2004.

[1] Aircraft observations of Asian outflow from the Transport and Chemical Evolution Over the Pacific (TRACE-P) aircraft mission over the NW Pacific (March and April 2001) show large CH<sub>4</sub> enhancements relative to background, as well as strong CH<sub>4</sub>-C<sub>2</sub>H<sub>6</sub>-CO correlations that provide signatures of regional sources. We apply a global chemical transport model simulation of the CH<sub>4</sub>-C<sub>2</sub>H<sub>6</sub>-CO system for the TRACE-P period to interpret these observations in terms of CH<sub>4</sub> sources and to explore in particular the unique constraints from the CH<sub>4</sub>-C<sub>2</sub>H<sub>6</sub>-CO correlations. We use as a priori a global CH<sub>4</sub> source inventory constrained with National Oceanic and Atmospheric Administration (NOAA) Climate Monitoring and Diagnostics Laboratory (CMDL) surface observations [Wang *et al.*, 2004]. We find that the observed CH<sub>4</sub> concentration enhancements and CH<sub>4</sub>-C<sub>2</sub>H<sub>6</sub>-CO correlations in Asian outflow in TRACE-P are determined mainly by anthropogenic emissions from China and Eurasia (defined here as Europe and eastern Russia), with only little contribution from tropical sources (wetlands and biomass burning). The a priori inventory overestimates the observed CH<sub>4</sub> enhancements and shows regionally variable biases for the CH<sub>4</sub>/C<sub>2</sub>H<sub>6</sub> slope. The CH<sub>4</sub>/CO slopes are simulated without significant bias. Matching both the observed CH<sub>4</sub> enhancements and the CH<sub>4</sub>-C<sub>2</sub>H<sub>6</sub>-CO slopes in Asian outflow requires increasing the east Asian anthropogenic source of CH<sub>4</sub>, and decreasing the Eurasian anthropogenic source, by at least 30% for both. The need to increase the east Asian source is driven by the underestimate of the CH<sub>4</sub>/C<sub>2</sub>H<sub>6</sub> slope in boundary layer Chinese outflow. The Streets *et al.* [2003] anthropogenic emission inventory for east Asia fits this constraint by increasing CH<sub>4</sub> emissions from that region by 40% relative to the a priori, largely because of higher livestock and landfill source estimates. Eurasian sources (mostly European) then need to be reduced by 30–50% from the a priori value of 68 Tg yr<sup>-1</sup>. The decrease of European sources could result in part from recent mitigation of emissions from coal mining and landfills. **INDEX TERMS:** 0322 Atmospheric Composition and Structure: Constituent sources and sinks; 0365 Atmospheric Composition and Structure: Troposphere—composition and chemistry; 0368 Atmospheric Composition and Structure: Troposphere—constituent transport and chemistry; **KEYWORDS:** methane, emissions, correlations

**Citation:** Xiao, Y., D. J. Jacob, J. S. Wang, J. A. Logan, P. I. Palmer, P. Suntharalingam, R. M. Yantosca, G. W. Sachse, D. R. Blake, and D. G. Streets (2004), Constraints on Asian and European sources of methane from CH<sub>4</sub>-C<sub>2</sub>H<sub>6</sub>-CO correlations in Asian outflow, *J. Geophys. Res.*, 109, D15S16, doi:10.1029/2003JD004475.

### 1. Introduction

[2] Atmospheric methane (CH<sub>4</sub>) is an important greenhouse gas with an atmospheric lifetime of ~10 years. The

atmospheric abundance of CH<sub>4</sub> has increased by a factor of 2.5 since preindustrial times [Etheridge *et al.*, 1998]. The resulting radiative forcing is half that of CO<sub>2</sub> [Hansen *et al.*, 2000]. Methane also plays a central role in atmospheric chemistry. It is an important sink for tropospheric OH and hence affects the oxidizing power of the atmosphere. It is a major source of tropospheric ozone, with implications for both the oxidizing power of the atmosphere and air quality [Fiore *et al.*, 2002]. Methane affects stratospheric ozone both by scavenging Cl radicals and by providing a source of water vapor. Better understanding of anthropogenic influences on CH<sub>4</sub> is essential for addressing issues of climate change and global atmospheric chemistry.

<sup>1</sup>Department of Earth and Planetary Sciences, Division of Engineering and Applied Sciences, Harvard University, Cambridge, Massachusetts, USA.

<sup>2</sup>Now at Environmental Defense, New York, USA.

<sup>3</sup>NASA Langley Research Center, Hampton, Virginia, USA.

<sup>4</sup>Department of Chemistry, University of California, Irvine, California, USA.

<sup>5</sup>Argonne National Laboratory, Argonne, Illinois, USA.

[3] Considerable research has focused on quantifying sources of  $\text{CH}_4$  [Intergovernmental Panel on Climate Control (IPCC), 2001]. The major anthropogenic sources include rice cultivation, livestock, landfills, fossil fuel production and consumption (natural gas venting, leakage, and coal mining), and biomass burning. The major natural sources include wetlands and termites. The total emission from all sources is known to be in the range  $460\text{--}600\text{ Tg yr}^{-1}$  because of independent constraints from halocarbon data on the global mean tropospheric OH concentration and hence on the  $\text{CH}_4$  sink [Prinn *et al.*, 1995, 2001; Spivakovsky *et al.*, 2000]. However, estimates for most of the individual source terms in the global  $\text{CH}_4$  budget have uncertainties of a factor of two or more according to IPCC [2001]. Better understanding of these individual source terms and their contributions to the long-term trend in  $\text{CH}_4$  is needed.

[4] The traditional approach for estimating  $\text{CH}_4$  sources has been by global extrapolation from limited flux measurements and socioeconomic data [e.g., Matthews and Fung, 1987; Matthews *et al.*, 1991; Lerner *et al.*, 1988; Cicerone and Oremland, 1988]. These bottom-up emission inventories suffer from substantial uncertainty due to undersampling of the sources and poor characterization of source variability. Global chemical transport model (CTM) simulations of atmospheric  $\text{CH}_4$  observations from the National Oceanic and Atmospheric Administration (NOAA) Climate Monitoring and Diagnostics Laboratory (CMDL) network of surface sites have been used to test the bottom-up emission inventories, either by a forward model with multiple scenarios [Fung *et al.*, 1991] or by formal inverse modeling methods [Hein *et al.*, 1997; Houweling *et al.*, 1999; Wang *et al.*, 2004; S. E. Mikaloff Fletcher *et al.*, Constraining  $\text{CH}_4$  source estimates with atmospheric observations of  $\text{CH}_4$  and its  $^{13}\text{C}/^{12}\text{C}$  isotopic ratios in  $\text{CH}_4$ : 1. Inverse modeling of source processes, submitted to *Global Biogeochemical Cycles*, 2004a, hereinafter referred to as Mikaloff Fletcher *et al.*, submitted manuscript, 2004a; S. E. Mikaloff Fletcher *et al.*, Constraining  $\text{CH}_4$  source estimates with atmospheric observations of  $\text{CH}_4$  and its  $^{13}\text{C}/^{12}\text{C}$  isotopic ratios in  $\text{CH}_4$ : 2. Inverse modeling of fluxes from geographical regions, submitted to *Global Biogeochemical Cycles*, 2004b, hereinafter referred to as Mikaloff Fletcher *et al.*, submitted manuscript, 2004b]. However, spatial overlap of the sources makes it difficult to derive a unique set of top-down constraints for  $\text{CH}_4$  sources from the limited surface air observations. Additional constraints on the  $\text{CH}_4$  budget and specific sources are provided by measurements of the carbon isotopes  $\delta^{13}\text{C}$  and  $^{14}\text{CH}_4$  [Lowe *et al.*, 1991, 1994; Gupta *et al.*, 1996; Quay *et al.*, 1999; Miller *et al.*, 2002; Mikaloff Fletcher *et al.*, submitted manuscript, 2004a; Mikaloff Fletcher *et al.*, submitted manuscript, 2004b], but these data are even more limited.

[5] We show here that improved top-down constraints on the sources of  $\text{CH}_4$  can be obtained from observations of  $\text{CH}_4\text{-C}_2\text{H}_6\text{-CO}$  correlations interpreted with a global CTM. Ground-based and aircraft measurements show strong correlations of  $\text{CH}_4$  with  $\text{C}_2\text{H}_6$  and CO [Harriss *et al.*, 1994; Blake *et al.*, 1996; Bartlett *et al.*, 1996; Shipham *et al.*, 1998; Matsueda and Inoue, 1999]. Ethane ( $\text{C}_2\text{H}_6$ ) is a tracer of natural gas leakage, coal mining, and biomass burning [Rudolph, 1995]. CO is a general tracer of combustion. Both

$\text{C}_2\text{H}_6$  and CO have atmospheric lifetimes of a few months, sufficiently long to serve as atmospheric tracers of their sources. One might therefore expect the biomass-burning source of  $\text{CH}_4$  to have a correlated  $\text{CH}_4\text{-C}_2\text{H}_6\text{-CO}$  signature; the natural gas/oil/coal mining sources to have a correlated  $\text{CH}_4\text{-C}_2\text{H}_6$  signature; and the sources from livestock, rice cultivation, landfills, and wetlands to have no direct correlations with CO and  $\text{C}_2\text{H}_6$ . In practice, collocation of these different sources complicates the interpretation, and a CTM analysis is needed.

[6] We focus our analysis here on  $\text{CH}_4\text{-C}_2\text{H}_6\text{-CO}$  correlations in Asian outflow, using observations from the NASA Transport and Chemical Evolution Over the Pacific (TRACE-P) aircraft mission over the western Pacific during March and April 2001 [Jacob *et al.*, 2003]. Asia is of particular interest as a source of  $\text{CH}_4$  owing to its large population, rapid industrialization, and extensive rice cultivation. There is also considerable seasonal biomass burning in Southeast Asia in spring [Duncan *et al.*, 2003]. The TRACE-P mission used two aircraft, based in Hong Kong and Japan, to characterize the chemical composition of Asian outflow. The major outflow pathways involved frontal lifting by warm conveyor belts (WCBs) ahead of southeastward moving cold fronts and boundary layer advection behind the cold fronts [Fuelberg *et al.*, 2003; Liu *et al.*, 2003]. Bartlett *et al.* [2003] reported strong correlations of  $\text{CH}_4$  with  $\text{C}_2\text{H}_6$ , ethyne ( $\text{C}_2\text{H}_2$ ), propane ( $\text{C}_3\text{H}_8$ ), and carbon tetrachloride ( $\text{C}_2\text{Cl}_4$ ) in the Asian outflow. They concluded that urban and combustion sources dominated the regional  $\text{CH}_4$  budget. However, a bottom-up inventory of Asian  $\text{CH}_4$  sources for 2000 generated by Streets *et al.* [2003] in support of TRACE-P identified livestock, landfills, rice cultivation, coal mining, and biomass burning as the principal regional sources of  $\text{CH}_4$ , in apparent contradiction with the analysis of Bartlett *et al.* [2003]. The Streets *et al.* [2003] inventory also includes estimates of  $\text{C}_2\text{H}_6$  and CO emissions, allowing a consistent interpretation of observed TRACE-P correlations using a CTM simulation.

[7] We use here the GEOS-CHEM CTM [Bey *et al.*, 2001] in a consistent simulation of the  $\text{CH}_4\text{-C}_2\text{H}_6\text{-CO}$  system for the TRACE-P period. This model has been used previously for global simulations of  $\text{CH}_4$  and CO aimed at understanding trends in the past decade [Wang *et al.*, 2004; B. N. Duncan *et al.*, Model study of the variability and trends of carbon monoxide (1988–1997): 1. Model formulation, evaluation, and sensitivity, submitted to *Journal of Geophysical Research*, 2004a; B. N. Duncan *et al.*, Model study of the variability and trends of carbon monoxide (1988–1997): 2. Trends and regulating factors, submitted to *Journal of Geophysical Research*, 2004b]; Previous GEOS-CHEM applications to the analysis of TRACE-P data included investigation of Asian outflow pathways [Liu *et al.*, 2003] and transpacific transport [Heald *et al.*, 2003b; Jaeglé *et al.*, 2003], as well as quantification of the Asian sources of CO [Palmer *et al.*, 2003a; Heald *et al.*, 2003a],  $\text{CO}_2$  (P. Suntharalingam *et al.*, Improved quantification of Chinese carbon fluxes using  $\text{CO}_2/\text{CO}$  correlations in Asian outflow, submitted to *Journal of Geophysical Research*, 2004, hereinafter referred to as Suntharalingam *et al.*, submitted manuscript, 2004), nitriles [Li *et al.*, 2003], halocarbons [Palmer *et al.*, 2003b], and ozone [Liu *et al.*, 2004]. Transport in the model is thus heavily diagnosed for

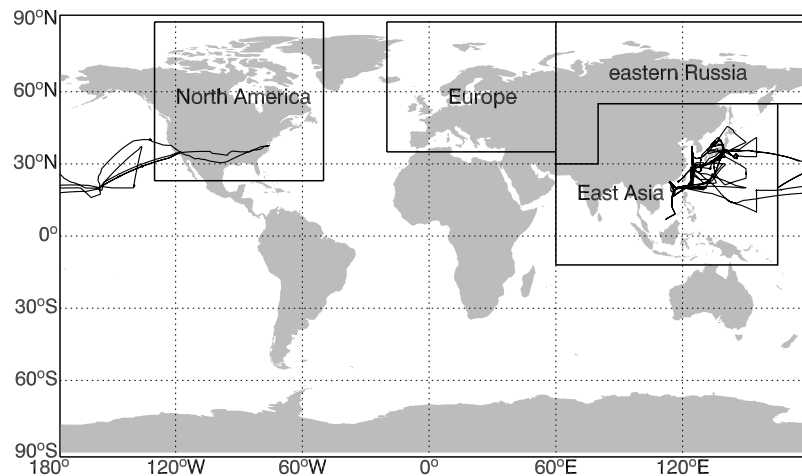


**Figure 1.** Tagged source regions for the  $\text{CH}_4$ ,  $\text{C}_2\text{H}_6$ , and  $\text{CO}$  simulations. “Eurasia” in the text refers to the combination of Europe and eastern Russia. The Transport and Chemical Evolution Over the Pacific (TRACE-P) flight tracks are also shown.

the TRACE-P period, and there are no systematic biases [Kiley *et al.*, 2003].

## 2. Model Description

### 2.1. General Description

[8] The GEOS-CHEM CTM (available at <http://www.as.harvard.edu/chemistry/trop/geos/index.html>, v4.26) is driven by assimilated meteorological fields from the Goddard Earth Observing System (GEOS) of the NASA Global Modeling and Assimilation Office (GMAO). We use GEOS-3 meteorological fields for the TRACE-P time period with a horizontal resolution of  $1^\circ \times 1^\circ$ , 48 vertical sigma levels up to 0.01hPa, and a temporal resolution of 6 hours (3 hours for surface variables and mixed layer depths). The horizontal resolution is degraded here to  $2^\circ$  latitude by  $2.5^\circ$  longitude for computational expediency.

[9] The main sinks of  $\text{CH}_4$ ,  $\text{CO}$ , and  $\text{C}_2\text{H}_6$  are reactions with OH. The rate constants are from DeMore *et al.* [1997]. For  $\text{CH}_4$  we also include a minor sink from soil absorption (about  $30 \text{ Tg yr}^{-1}$ ) [Wang *et al.*, 2004]. Global three-dimensional (3-D) monthly mean tropospheric OH concentrations from a full tropospheric oxidant simulation (GEOS-CHEM v4.33) are used [Fiore *et al.*, 2003]. These OH concentrations yield an annual mean methyl chloroform ( $\text{CH}_3\text{CCl}_3$ ) lifetime against loss by tropospheric OH of 6.3 years, which is within the range of 5.3–6.9 years estimated by Prinn *et al.* [2001] from  $\text{CH}_3\text{CCl}_3$  measurements. The same OH fields have been used in other GEOS-CHEM simulations of the TRACE-P data [Li *et al.*, 2003; Heald *et al.*, 2003a, 2003b; Jaeglé *et al.*, 2003; Palmer *et al.*, 2003a].

[10] Tagged tracer simulations for  $\text{CH}_4$ ,  $\text{C}_2\text{H}_6$ , and  $\text{CO}$  in GEOS-CHEM are conducted to quantify the contributions to atmospheric concentrations from different source regions and source types. These tagged tracer simulations all use the same OH concentrations as the standard simulation so that results are additive. Source regions include east Asia, Europe, eastern Russia, North America, and the rest of the world as defined in Figure 1. We will refer to “Eurasia” as the combination of Europe and eastern Russia. Source types

for  $\text{CH}_4$  include livestock, rice cultivations, wetlands, biomass burning, biofuel, fossil fuel (gas/oil/coal mining), and landfills. The simulations of  $\text{C}_2\text{H}_6$  and  $\text{CO}$  are initialized with a 2-year spin-up. The initialization of the  $\text{CH}_4$  simulation is described in section 2.3.

### 2.2. Emissions

#### 2.2.1. Methane

[11] We use the global 1998 inventory of Wang *et al.* [2004] as our a priori estimate of  $\text{CH}_4$  emissions. The global  $\text{CH}_4$  growth rate was near zero between 1998 and 2001, presumably reflecting a leveling-off of emissions [Dlugokencky *et al.*, 1998], although a positive trend of global OH concentrations could have contributed. Wang *et al.* [2004] originally derived their inventory for 1994 by inverse analysis of the NOAA/CMDL surface observations, using GEOS-CHEM as the forward model, and then applied interannual variability to these emissions for 1988–1998 on the basis of socioeconomic and meteorological data. They found that they could capture in this manner much of the observed spatial and temporal variability of  $\text{CH}_4$  concentrations over the 1988–1997 decade.

[12] Table 1 summarizes the global and east Asian  $\text{CH}_4$  sources from Wang *et al.* [2004] and compares them with the global EDGAR3.2 emission inventory [Olivier and Berdowski, 2001] and to the east Asian emission inventory of Streets *et al.* [2003]. The latter two inventories include only anthropogenic sources and biomass burning. Anthropogenic sources here include rice cultivation, livestock, fossil fuel (gas/oil/coal mining), landfills, and biofuel. Classifying the biomass-burning source as natural or anthropogenic is somewhat subjective. For the purpose of this paper we will regard it as natural, largely out of convenience since its geographical distribution (mainly tropical) is distinct from that of the major anthropogenic sources. Annual east Asian emissions in the Wang *et al.* [2004] inventory are dominated by wetlands, rice cultivation, livestock (including animal enteric fermentation and animal waste management), coal mining, and landfills. Natural gas and biofuel sources are relatively small. We refer to the sum of natural gas (production and transmission), oil (production, trans-

**Table 1.** East Asian<sup>a</sup> and Global CH<sub>4</sub> Emissions (Tg yr<sup>-1</sup>)

	<i>Wang et al.</i> [2004] <sup>b</sup> , Year 1998		<i>Streets et al.</i> [2003] <sup>c</sup> , Year 2000	<i>Olivier and Berdowski</i> [2001] (EDGAR3.2) <sup>e</sup> , Year 1995	
	East Asia <sup>d</sup>	Globe		East Asia	Globe
Total anthropogenic	113	286	106	117	284
Rice cultivation	52(40%)	59	24	36	39
Livestock	27	83	36	28	89
Fossil fuel					
Coal mining	14	31	8	14	33
Gas/oil	4.8	52	5.8	6.6	53
Landfills	9.7	50	23	21	56
Biofuel	5.8	9.2	8.6	8.3	14
Total natural	45	231	–	–	–
Biomass burning	4.3(240%)	21	3.1	1.8	13
Wetlands	36(80%)	185	–	–	–
Termites	4.6	25	–	–	–

<sup>a</sup>Including India (see Figure 1).

<sup>b</sup>Used as a priori in this work.

<sup>c</sup>These inventories include only anthropogenic sources and biomass burning.

<sup>d</sup>Percentages in parentheses are the seasonal scaling factors for February to April 2001 (TRACE-P period) relative to the annual mean. For example, the value of 40% for rice cultivation means that the emissions in February to April are only 40% of the annual mean value.

mission, and handling), and coal mining as the fossil fuel source. The other fossil fuel sources of CH<sub>4</sub> from industry, power generation, residential and commercial use, and transport are all minor [Olivier and Berdowski, 2001].

[13] East Asian emissions from rice cultivation in the Streets et al. [2003] inventory are 50% lower than in the work of Wang et al. [2004] and the coal mining source is 40% lower, while livestock emissions are 30% higher and landfill emissions are a factor of two higher. The EDGAR3.2 inventory is better aligned with Streets et al. [2003].

[14] Seasonal variation of CH<sub>4</sub> emissions from rice cultivation, biomass burning, and wetlands is applied here following Wang et al. [2004]. Our focus is on the February to April (TRACE-P) period. East Asian emissions from rice cultivation peak in June to October (170% of annual mean flux) and are low during February to April (40% of annual mean flux). This is consistent with the Streets et al. [2003] inventory, in which CH<sub>4</sub> emissions from rice cultivation peak in fall and are low in spring. Emissions from natural wetlands in February to April are about 80% of the annual average. Biomass burning in Southeast Asia is by contrast at its seasonal high (240% of annual mean flux) during February to April.

[15] Figure 2 shows the geographical distribution of CH<sub>4</sub> emissions for February to April 2001 in the Wang et al. [2004] inventory. There are important regional differences between sources. In China and India the major sources are livestock, coal mining, landfills, and rice cultivation. Landfills and gas/oil are the main sources in Japan. Wetlands, rice cultivation, biomass burning, and livestock are important sources in Southeast Asia. Fossil fuel (mostly from natural gas), landfills, and livestock are dominant in Eurasia.

### 2.2.2. Ethane

[16] Major sources of C<sub>2</sub>H<sub>6</sub> include natural gas leakage, natural gas venting, coal mining, biofuel use, and biomass burning [Rudolph, 1995]. We refer to the sum of the first three sources as the fossil fuel source. Anthropogenic emissions (fossil fuel and biofuel) for east Asia are taken from Streets et al. [2003]. Fossil fuel emissions for the rest

of the world are scaled to the corresponding source of CH<sub>4</sub>, for which better a priori information is available. Biofuel emissions for the rest of the world are based on the Yevich and Logan [2003] biofuel inventory with emission factors from Andreae and Merlet [2001]. Biomass burning emissions are scaled to the corresponding emission of CO [Duncan et al., 2003], with a C<sub>2</sub>H<sub>6</sub>/CO emission ratio dependent on fuel type [Staudt et al., 2003].

[17] Natural gas composition varies with geographical region [Rudolph, 1995]. In this work, CH<sub>4</sub>/C<sub>2</sub>H<sub>6</sub> emission factors for the fossil fuel sources outside east Asia were derived by fitting the global C<sub>2</sub>H<sub>6</sub> simulation to atmospheric concentration data including surface sites, ship cruises, aircraft missions, and total columns from ground-based remote sensing. We thus adopt molar CH<sub>4</sub>/C<sub>2</sub>H<sub>6</sub> emission ratios from fossil fuel of 8 in eastern Russia, 24 in Europe, and 19 for the rest of the world except east Asia, where the use of Streets et al. [2003] inventory for C<sub>2</sub>H<sub>6</sub> yields a molar CH<sub>4</sub>/C<sub>2</sub>H<sub>6</sub> emission ratio of 40. These values are highly variable but roughly in the range of U.S. energy industry data [Flores et al., 1999], which indicate emission ratios of 38 or higher (dry gas), 19–37 (gas condensate), and 11–18 (oil). Measurements in Chinese cities indicate CH<sub>4</sub>/C<sub>2</sub>H<sub>6</sub> concentration ratios in the range of 5–35 (D. R. Blake, unpublished data, 2001). Our total global C<sub>2</sub>H<sub>6</sub> source of 13.5 Tg yr<sup>-1</sup> (Table 2) is consistent with previous literature estimates of 8–24 Tg yr<sup>-1</sup> [Blake and Rowland, 1986; Kanakidou et al., 1991; Rudolph, 1995; Boissard et al., 1996; Gupta et al., 1998; Wang et al., 1998].

### 2.2.3. Carbon Monoxide

[18] Our CO simulation for the TRACE-P period is that of Palmer et al. [2003a], who conducted an inverse model analysis of Asian CO sources on the basis of the TRACE-P CO observations. They used a priori inventories from Streets et al. [2003] for east Asian anthropogenic sources (fossil fuel and biofuel combustion), Heald et al. [2003a] for biomass burning in Southeast Asia, and Duncan et al. [2003] for other sources. Transport was simulated with GEOS-CHEM, which served as the forward model for the inversion. Fitting the CO observations in TRACE-P

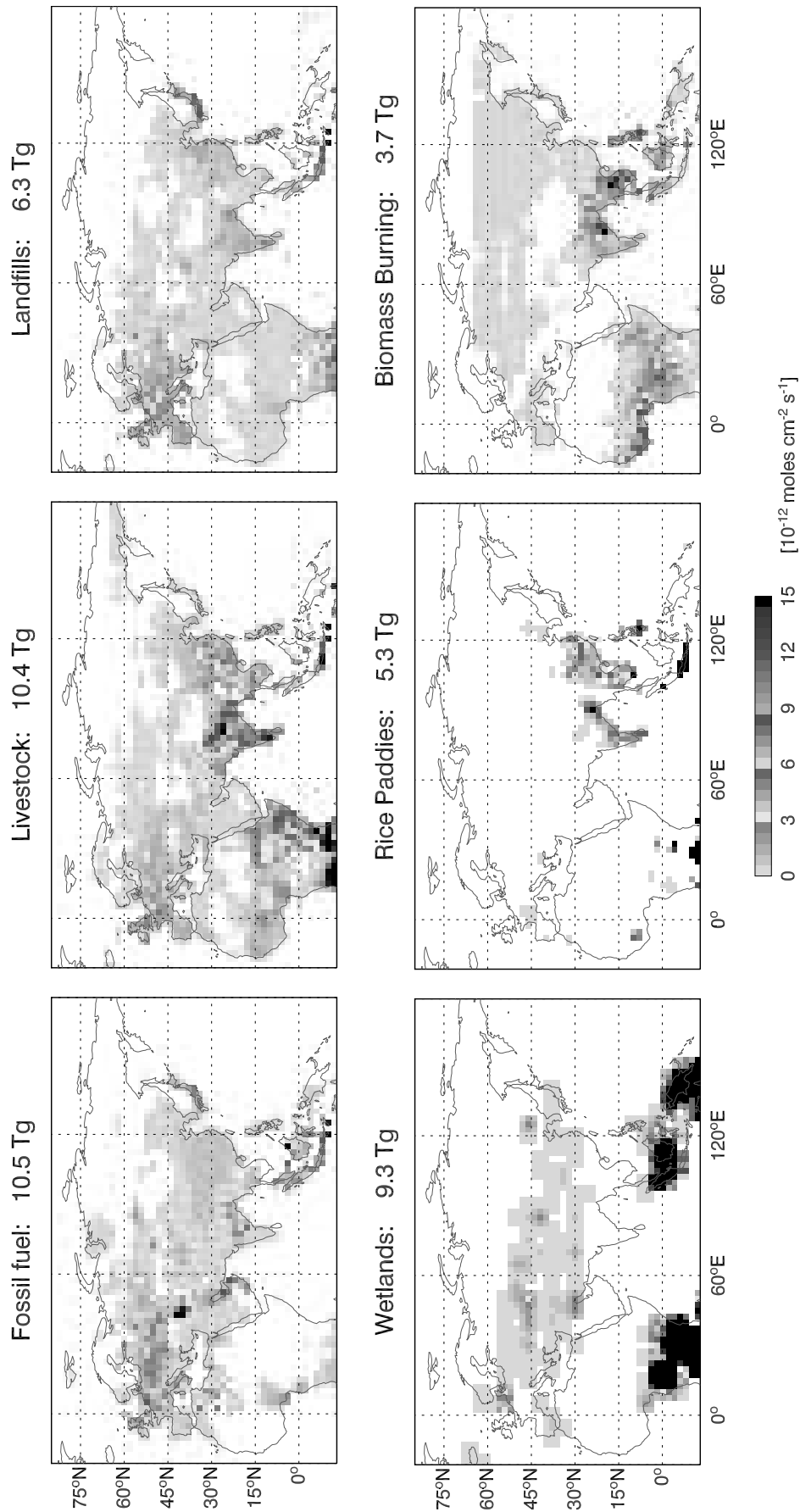


**Figure 2.** Distribution of CH<sub>4</sub> sources for the TRACE-P period (February to April, 2001) based on Wang *et al.* [2004] and used as a priori in this work. Total emissions from east Asian and Eurasian sources over the 3-month period are indicated for each source on the top of the corresponding panel. See color version of this figure at back of this issue.

**Table 2.** CH<sub>4</sub>-C<sub>2</sub>H<sub>6</sub>-CO Emissions and Emission Ratios for February to April 2001<sup>a</sup>

	Global			East Asia <sup>b</sup>				Eurasia <sup>c</sup>	
	Fossil Fuel	Biofuel	Biomass Burning	Fossil Fuel	Biofuel	Biomass Burning	All Anthropogenic Sources <sup>d</sup>	Fossil Fuel	All Anthropogenic Sources <sup>d</sup>
CH <sub>4</sub> , Tg	21	2.3	6.8	3.6	0.93	0.95	12	7.7	15
C <sub>2</sub> H <sub>6</sub> , Tg	2.1	0.51	0.62	0.17	0.18	0.051	0.35	0.72	0.79
CO, Tg	80	42	110	21	16	13.4	37	22	27
CH <sub>4</sub> /C <sub>2</sub> H <sub>6</sub> , molar	19	8.5	20	40	10	35	64	20	37
CH <sub>4</sub> /CO, molar	0.46	0.10	0.11	0.30	0.10	0.12	0.57	0.62	1.0
C <sub>2</sub> H <sub>6</sub> /CO, 10 <sup>-3</sup> molar	25	11	5.3	7.6	10	3.6	8.8	31	27

<sup>a</sup>Total emissions for the 3-month period. CH<sub>4</sub> emissions are from Wang *et al.* [2004] (section 2.2.1) and are used here as our a priori. C<sub>2</sub>H<sub>6</sub> sources are as described in section 2.2.2. CO emissions are from Palmer *et al.* [2003a] (section 2.2.3). Emission ratios are calculated from the emission totals in the table.

<sup>b</sup>Excluding India.

<sup>c</sup>Including Europe and eastern Russia (see Figure 1).

<sup>d</sup>Including contributions from rice cultivation, livestock, fossil fuel, landfill, and biofuel emissions.

required a 54% increase in anthropogenic emissions from China relative to the a priori, constrained by the observations in boundary layer outflow, and a 74% decrease in emissions from Southeast Asia (mostly from biomass burning), constrained by the observations in the free troposphere south of 30°N. Similar results for CO emissions were obtained by Heald *et al.* [2003b] from an analysis of Measurements of Pollution in the Troposphere (MOPITT) satellite observations of CO columns during the TRACE-P period. The optimized a priori sources of CO from Palmer *et al.* [2003a] are given in Table 2. The resulting simulation of CO concentrations, which we use here, is compared with TRACE-P observations in that paper. The mean bias is -4 ppb and the frequency distribution of differences is peaked around zero.

#### 2.2.4. Emission Ratios

[19] Table 2 gives the CH<sub>4</sub>-C<sub>2</sub>H<sub>6</sub>-CO emission ratios from selected sources, globally and for the two main source regions contributing to the structure of Asian outflow over the Pacific during TRACE-P: east Asia and Eurasia (Europe and eastern Russia). We exclude India from east Asia here, since India did not contribute significantly to the structure of Asian outflow during the TRACE-P period [Palmer *et al.*, 2003a]. There is substantial spatial overlap between the different anthropogenic sources of CH<sub>4</sub> (Figure 2); hence we also give for each region in Table 2 the lumped anthropogenic emission ratio.

[20] Within east Asia, the CH<sub>4</sub>/C<sub>2</sub>H<sub>6</sub> emission ratio for fossil fuel (40 molar) is higher than that for biofuel (10) and close to that for biomass burning (35). The C<sub>2</sub>H<sub>6</sub> emission factor for biofuel is much higher than for open biomass burning [Bertschi *et al.*, 2003], apparently because of p ethane production during flaming combustion [Yokelson *et al.*, 2003]. The CH<sub>4</sub>/CO emission ratio for fossil fuel (0.30 molar) is 2–3 times that for biofuel (0.10) and biomass burning (0.12). The C<sub>2</sub>H<sub>6</sub>/CO emission ratio from fossil fuel ( $7.6 \times 10^{-3}$  molar) is lower than that for biofuel ( $10 \times 10^{-3}$ ) but much higher than that for biomass burning ( $3.6 \times 10^{-3}$ ). The CH<sub>4</sub>/CO and CH<sub>4</sub>/C<sub>2</sub>H<sub>6</sub> emission ratios from all lumped anthropogenic sources are larger than those from the combustion sources owing to additional CH<sub>4</sub> inputs from livestock, landfills, and rice cultivation.

[21] The CH<sub>4</sub> and C<sub>2</sub>H<sub>6</sub> anthropogenic emissions from Eurasia are larger than from east Asia while the CO source

is much smaller, reflecting more vigorous pollution control of CO and greater natural gas production in Eurasia. There are thus large differences in the CH<sub>4</sub>/CO and C<sub>2</sub>H<sub>6</sub>/CO emission ratios for anthropogenic sources from east Asia versus Eurasia (0.57 versus 1.0 for CH<sub>4</sub>/CO,  $8.8 \times 10^{-3}$  versus  $27 \times 10^{-3}$  molar for C<sub>2</sub>H<sub>6</sub>/CO), and the CH<sub>4</sub>/C<sub>2</sub>H<sub>6</sub> anthropogenic emission ratio is larger for east Asia (64 versus 37).

#### 2.3. Initialization and Global Aspects of the CH<sub>4</sub> Simulation

[22] Proper model initialization of the CH<sub>4</sub> tagged tracers presents a difficulty because of the long lifetime of CH<sub>4</sub>. We wish to use these tracers to interpret the variability of CH<sub>4</sub> in Asian outflow during March and April 2001. Because the timescale for mixing within the Northern Hemisphere is a few months, we expect the variability observed in TRACE-P to reflect fresh emissions from the past 2–3 months together with the latitudinal and vertical structure of the background. Accordingly, we define a background CH<sub>4</sub> tracer in the simulation as the CH<sub>4</sub> present in the atmosphere on 1 January 2001, including contributions from all sources. This background tracer has no emissions following 1 January and is allowed to decay by oxidation by OH. The other tagged tracers, representing different CH<sub>4</sub> source regions and source types, are initialized with zero concentration on 1 January. They build up over the course of the simulation as a result of emissions and are removed by oxidation by OH. The same archived OH concentration fields are used to calculate the losses of all tracers; hence the sum of the individual tracers adds up to the total CH<sub>4</sub> concentration.

[23] We need to define a global field for the background tracer on 1 January 2001. We start from NOAA/CMDL global surface observations for December 2000 (available at <ftp://ftp.cmdl.noaa.gov>) [Dlugokencky *et al.*, 1994, 2001] to define the latitudinal gradient of CH<sub>4</sub> concentrations at the surface. From this initial state with no vertical gradients in the troposphere, we conduct a 2-year spin-up simulation with 2000 meteorological fields and the Wang *et al.* [2004] emissions to construct the vertical and longitudinal gradients of CH<sub>4</sub>. The results from this 2-year spin-up are then scaled globally with a uniform factor to optimize agreement with the NOAA/CMDL surface data for December 2000.

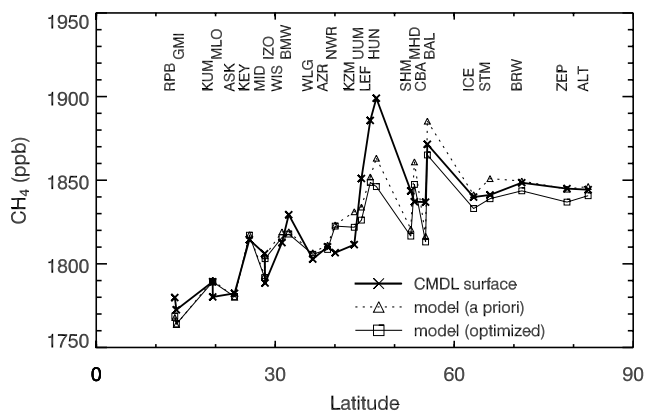


**Figure 3.** Simulated versus observed latitudinal gradient of monthly mean  $\text{CH}_4$  surface concentrations in March 2001 at the National Oceanic and Atmospheric Administration (NOAA) Climate Monitoring and Diagnostics Laboratory (CMDL) surface sites north of  $10^\circ\text{N}$  (available at ftp://ftp.cmdl.noaa.gov). The CMDL station code is displayed. Observations (bold solid line with crosses) are compared with model values using the a priori (dotted line with triangles) and optimized (solid line with squares) emission inventories. The a priori emission inventory is from Wang *et al.* [2004]. The optimized emission inventory fit to the TRACE-P data uses regional anthropogenic emissions from Streets *et al.* [2003] for east Asia and Eurasian anthropogenic emissions reduced by 50% from the Wang *et al.* [2004] inventory.

[24] Evaluation of the model background for the TRACE-P period is shown in Figure 3 by comparison of model results for March 2001 with observations from NOAA/CMDL sites. The model reproduces the latitudinal gradient in the background without bias over the range of interest ( $10\text{--}50^\circ\text{N}$ ), except at a few continental sites around  $45^\circ\text{N}$  (LEF, HUN) where observed concentrations are high due to local source influence. Simulation of vertical gradients is discussed below using the TRACE-P observations.

### 3. Model Simulation of TRACE-P Observations

[25] We first examine the ability of the model driven by a priori sources from the Wang *et al.* [2004] inventory (Table 1) to reproduce the general features of the  $\text{CH}_4$  distributions and  $\text{CH}_4\text{-C}_2\text{H}_6\text{-CO}$  correlations observed in TRACE-P. The TRACE-P  $\text{CH}_4$  measurements rely on the same calibration standards as NOAA/CMDL so that  $\text{CH}_4$  concentrations should be consistent across the two data sets. We will show also results from a simulation where the Streets *et al.* [2003] anthropogenic emissions for  $\text{CH}_4$  in east Asia have been superimposed on the Wang *et al.* [2004] inventory. The ability of the model to simulate  $\text{C}_2\text{H}_6$  observations using the sources in Table 2 will also be examined. A similar evaluation for  $\text{CO}$ , also using the sources of Table 2, was presented by Palmer *et al.* [2003a] and is not reported here. Throughout this paper, the model values are sampled along the flight tracks and the observations are averaged over model grid boxes. Stratospheric data ( $\text{O}_3 > 100$  ppb with  $\text{CO} < 100$  ppb) are excluded. The observations are averaged over model grid boxes, corresponding to an averaging time

span of 10–30 min for typically aircraft speeds. The model results are output every 3 hours. Considering that we are looking at aged air masses, at least 1 day downwind of the sources, the time discrepancy between the model and observation should be negligible. Linear regressions use the RMA (reduced major axis) method [Hirsch and Gilroy, 1984], accounting for errors in both variables.

#### 3.1. Methane

[26] Figure 4a (top) compares the simulated and observed  $\text{CH}_4$  concentrations for the ensemble of TRACE-P observations over the NW Pacific (west of  $160^\circ\text{E}$ ). The simulation shows strong correlation with observations ( $r^2 = 0.71$ ). The 6% positive bias (slope of the RMA regression line) is driven by boundary layer Asian outflow rather than by the background. This structure in the bias is more apparent in Figure 4b, which shows the simulated versus observed mean vertical gradients of  $\text{CH}_4$  concentrations in TRACE-P west of  $160^\circ\text{E}$ . Model results using the Streets *et al.*

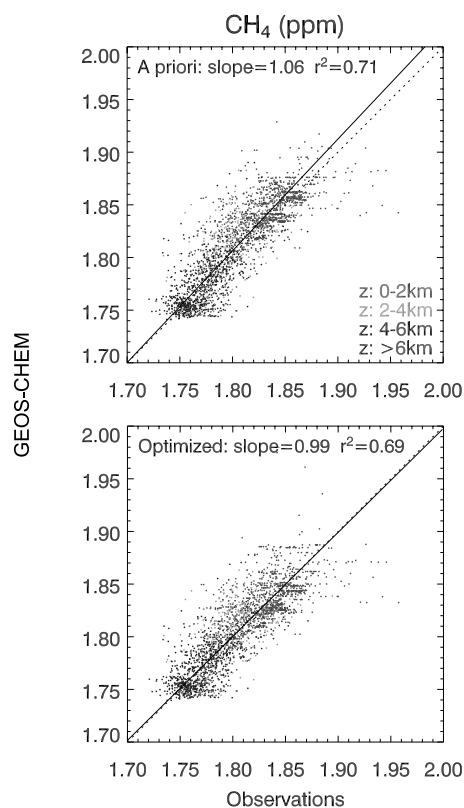


**Figure 4a.** Simulated versus observed concentrations of  $\text{CH}_4$  along the TRACE-P flight tracks over the northwest Pacific (west of  $160^\circ\text{E}$ ). Model results are shown for simulations with a priori (upper) and optimized (lower) emission inventories for  $\text{CH}_4$ . The model is sampled along the flight tracks, and the observations are averaged over the model grid boxes. The 1:1 line is shown as dotted. The solid line is the reduced major axis (RMA) regression line. The a priori emission inventory is from Wang *et al.* [2004]. The optimized emission inventory uses east Asian anthropogenic emissions from Streets *et al.* [2003] and Eurasian anthropogenic emissions decreased by 50% from the Wang *et al.* [2004] inventory. See color version of this figure at back of this issue.

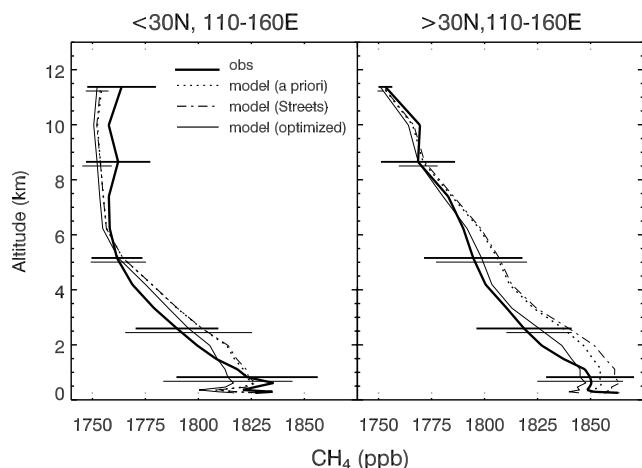


**Figure 4b.** Mean vertical profiles of  $\text{CH}_4$  concentrations along the TRACE-P flight tracks, north of  $30^{\circ}\text{N}$  and south of  $30^{\circ}\text{N}$  at  $110^{\circ}\text{E}$  to  $160^{\circ}\text{E}$  (NW Pacific, Asian outflow). Observations (thick lines) are compared with model values using the a priori emission inventory (dotted lines), the a priori inventory with anthropogenic east Asian sources from Streets *et al.* [2003] superimposed (dash-dotted lines), and the optimized emission inventory (solid lines). The a priori emission inventory is from Wang *et al.* [2004]. The optimized emission inventory uses east Asian anthropogenic emissions from Streets *et al.* [2003] and Eurasian anthropogenic emissions decreased by 50% from the Wang *et al.* [2004] inventory. The error bars show standard deviations ( $1\sigma$ ) for the observations and the optimized model at selected levels.

[2003] east Asian inventory are also shown. We distinguish between data north of  $30^{\circ}\text{N}$ , where anthropogenic outflow was strongest, and south of  $30^{\circ}\text{N}$ , where most of the Southeast Asian biomass burning influence was observed [Palmer *et al.*, 2003a]. The model results with a priori sources show positive bias in the simulation of the Asian outflow enhancement at 0–6 km altitude, particularly north of  $30^{\circ}\text{N}$ . The bias is larger when the Streets *et al.* [2003] inventory is used owing to higher livestock and landfill emissions in that inventory. Rice emissions are lower in the Streets *et al.* [2003] inventory than in the work of Wang *et al.* [2004], resulting in total annual east Asian  $\text{CH}_4$  emissions that are similar between the two inventories (Table 1). However, the rice emissions are at low latitudes (Figure 2) and are also at their seasonal minimum in February to April, thus making little contribution to the Asian outflow observed in TRACE-P. Although it would seem from Figure 4b that the Streets *et al.* [2003] inventory degrades the simulation, we will show in section 4 that using that inventory in combination with a decrease in Eurasian emissions provides in fact a good fit to  $\text{CH}_4$  concentrations for the TRACE-P period.

[27] Figure 4c (left) compares simulated and observed  $\text{CH}_4$  concentrations west of  $160^{\circ}\text{E}$  as a function of latitude and at different altitudes. Also shown (dashed lines) is the contribution of the  $\text{CH}_4$  background (emitted before 1 January 2001) to the model fields. The model reproduces the general increasing trend of  $\text{CH}_4$  with latitude, reflecting

both the background and the Asian outflow enhancements. The model underestimates observations south of  $16^{\circ}\text{N}$ , but these are mainly from a single flight over the South China Sea (Figure 1), which makes interpretation difficult.  $\text{CH}_4$  enhancements above the background in the model fields (difference between solid and dashed lines) reflect emissions over the January to April 2001 period. As shown in Figure 4c (right), we find that east Asian sources contribute most of this enhancement south of  $35^{\circ}\text{N}$ , while Eurasian sources (Europe and eastern Russia; the former is about 80%) dominate north of  $35^{\circ}\text{N}$ . The principal east Asian sources contributing to the enhancements below 4 km are livestock, landfills, and coal mining. The principal Eurasian sources contributing to the Asian outflow are natural gas, landfills, and livestock. Biomass burning in Southeast Asia is a relatively large source south of  $30^{\circ}\text{N}$ , mostly above 8 km (convective outflow), and at 2–4 km (WCB frontal outflow), consistent with TRACE-P observations for the HCN and  $\text{CH}_3\text{CN}$  biomass burning tracers [Li *et al.*, 2003; Singh *et al.*, 2003]. The wetlands source of  $\text{CH}_4$  does not contribute significantly to the Asian outflow sampled in TRACE-P because it is located too far south (see Figure 2).

### 3.2. Ethane

[28] Comparisons of simulated and observed  $\text{C}_2\text{H}_6$  concentrations are shown in Figure 5a (scatterplot), Figure 5b (vertical profiles), and Figure 5c (latitudinal gradients). There is strong correlation in the ensemble of data ( $r^2 = 0.73$ ). The regression slope of 1.04 in the scatterplot (Figure 5a) is mainly driven by the underestimate of the background. The magnitude of the enhancement in Asian outflow is well described, as shown in Figure 5b. The latitudinal gradients are similar to those of  $\text{CH}_4$ , and there is no distinct bias in the model for any of the major features. The Eurasian fossil fuel source makes the largest contribution to the model fields at all altitudes north of  $30^{\circ}\text{N}$ . East Asian sources make only a minor contribution north of  $30^{\circ}\text{N}$  but are relatively more important to the south, where the Eurasian influence is less.

### 3.3. $\text{CH}_4$ - $\text{C}_2\text{H}_6$ -CO Correlations

[29] We saw in section 3.1 that the model with a priori sources reproduces the general latitudinal and vertical distributions of  $\text{CH}_4$  in TRACE-P but is too high in the lower tropospheric Asian outflow. We will now examine what additional insights can be obtained from the observed  $\text{CH}_4$ - $\text{C}_2\text{H}_6$ -CO correlations. Observed pollution plumes with CO concentrations greater than 325 ppb on a 5-min average basis (4% of the data in all) are removed from the correlation analysis because they would otherwise overly influence the least squares statistics. We employ the bootstrap method [Venables and Ripley, 1999] to calculate the standard deviations of the slopes of the regression lines.

[30] Figure 6 compares the simulated and observed  $\text{CH}_4$ - $\text{C}_2\text{H}_6$ -CO correlations for regional subsets of the TRACE-P data. The slopes of the regression lines and associated standard deviations are given in Table 3. We will use the  $\text{CH}_4$ - $\text{C}_2\text{H}_6$  and  $\text{CH}_4$ -CO correlations as constraints on  $\text{CH}_4$  sources, and the  $\text{C}_2\text{H}_6$ -CO correlation to test the relative influence of east Asian and Eurasian sources. The region north of  $30^{\circ}\text{N}$  and below 2 km (“Chinese outflow”) sampled anthropogenic outflow but was largely devoid of biomass

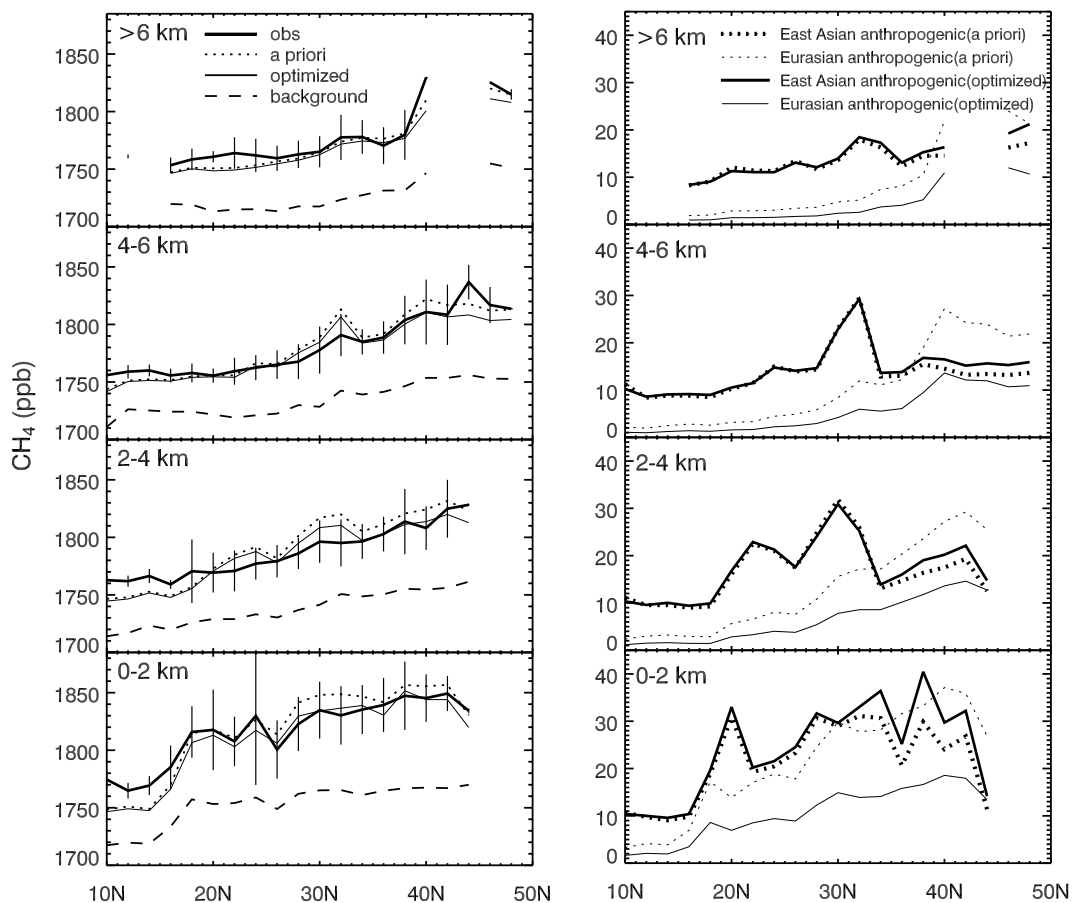


**Figure 4c.** (left) Latitudinal dependence of  $\text{CH}_4$  concentrations along the TRACE-P flight tracks west of  $160^\circ\text{E}$  and at different altitudes. Observations (thick lines) are compared with model results using a priori sources (dotted) and optimized sources (solid). Dashed lines indicate background  $\text{CH}_4$  in the model (see text). The error bars represent standard deviations for the observations. (right) Contributions from the anthropogenic east Asian and Eurasian tagged tracers to the  $\text{CH}_4$  model fields using the a priori (dotted) and the optimized (solid) emission inventories. The a priori emission inventory is from Wang *et al.* [2004]. The optimized emission inventory uses east Asian anthropogenic emissions from Streets *et al.* [2003] and Eurasian anthropogenic emissions decreased by 50% from the Wang *et al.* [2004] inventory.

burning influence [Liu *et al.*, 2003; Palmer *et al.*, 2003a; Russo *et al.*, 2003; Singh *et al.*, 2003]. The region south of  $30^\circ\text{N}$  and below 2 km (“tropical Asian outflow”) has more influence of sources from the tropical Asian region. In order to obtain independent information on Japanese/Korean sources, we use data from DC-8 flight 17 (31 March), which sampled a mix of Japanese and Korean influences but with relatively little Chinese influence [Blake *et al.*, 2003; Suntharalingam *et al.*, submitted manuscript, 2004]. Finally, we also examine the correlations in background air (east of  $160^\circ\text{E}$  and 2–8 km altitude).

[31] For Chinese outflow (Figure 6a and Table 3), the simulated  $\text{CH}_4/\text{CO}$  and  $\text{C}_2\text{H}_6/\text{CO}$  slopes are consistent with observations, while the  $\text{CH}_4/\text{C}_2\text{H}_6$  slope is significantly too low ( $39 \pm 1.1$  versus  $43 \pm 1.2 \times 10^{-3}$  molar). The  $\text{CH}_4$  and  $\text{C}_2\text{H}_6$  concentrations in Chinese outflow reflect contributions from anthropogenic sources in both east Asia and Eurasia (section 3.1 and 3.2). Correction of the  $\text{CH}_4/\text{C}_2\text{H}_6$  bias will be discussed in section 4.

[32] For tropical Asian outflow (Figure 6b) the observed  $\text{CH}_4/\text{CO}$  and  $\text{C}_2\text{H}_6/\text{CO}$  slopes are higher than for Chinese

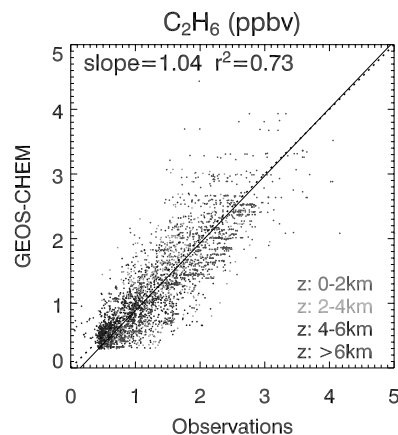


**Figure 5a.** Simulated versus observed concentrations of  $\text{C}_2\text{H}_6$  along the TRACE-P flight tracks over the northwest Pacific (west of  $160^\circ\text{E}$ ). The observations are averaged over the model grid boxes. The 1:1 line is shown as dotted. The solid line is the RMA regression line. See color version of this figure at back of this issue.

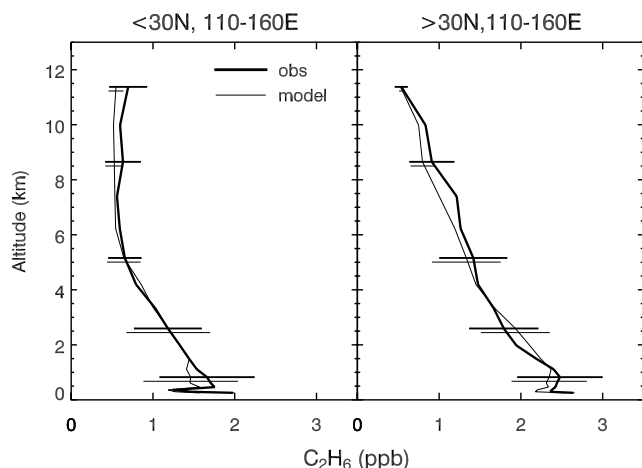


**Figure 5b.** Mean vertical profiles of  $C_2H_6$  concentrations along the TRACE-P flight tracks, north of  $30^\circ N$  and south of  $30^\circ N$  at  $110^\circ E$  to  $160^\circ E$  (NW Pacific, Asian outflow). Observations (thick lines) are compared with model values (solid lines). The error bars show the standard deviations for the observations and the model at selected levels.

outflow (0.46 versus 0.38 for  $CH_4/CO$ , 11 versus  $8.5 \times 10^{-3}$  molar for  $C_2H_6/CO$ ) while the  $CH_4/C_2H_6$  slopes are similar (42 versus 43). As shown by the tagged  $CH_4$  simulation, tropical  $CH_4$  sources from wetlands and biomass burning are of little importance and anthropogenic sources of  $CH_4$  from east Asia and Eurasia remain dominant in this region. The model captures the regional differences in the  $CH_4/CO$  and  $C_2H_6/CO$  slopes. However, it overestimates the  $CH_4/C_2H_6$  and  $CH_4/CO$  slopes significantly.

[33] Compared with the Chinese and tropical Asian outflow, the Japanese/Korean plumes (Figure 6c) feature significantly higher  $CH_4/C_2H_6$  slopes (45 versus 42–43),  $CH_4/CO$  (0.65 versus 0.38–0.46), and  $C_2H_6/CO$  ( $14$  versus  $9$ – $11 \times 10^{-3}$  molar). These regional differences are due to CO emission controls and to low biofuel emissions (characterized by a low  $CH_4/C_2H_6$  emission ratio). Again, the model captures this regional variation. It overestimates the  $CH_4/C_2H_6$  slope and underestimates the  $C_2H_6/CO$  slope, with no significant bias in the  $CH_4/CO$  slope (Table 3).

[34] Figure 6d shows the  $CH_4$ – $C_2H_6$ –CO correlations in background air masses east of  $160^\circ E$ . The observed slopes are much higher (58 for  $CH_4/C_2H_6$ , 0.75 for  $CH_4/CO$ , and  $13 \times 10^{-3}$  molar for  $C_2H_6/CO$ ) than in Asian outflow. These correlations reflect the common large-scale latitudinal gradients of the three gases. The model reproduces all these correlations without significant bias.

#### 4. Optimization of $CH_4$ Sources

[35] We have shown that both east Asian and Eurasian anthropogenic sources were major contributors to the  $CH_4$  enhancement in Asian outflow observed in TRACE-P and that the correlations of  $CH_4$  with  $C_2H_6$  and CO have distinct characteristics related to both regional sources and background. We seek now to use the constraints from the observed  $CH_4$  enhancements and  $CH_4$ – $C_2H_6$ –CO correlations to optimize the representation of  $CH_4$  sources in the model in a forward fashion. Considering that the  $C_2H_6$  and CO simu-

lations match the observations closely (see section 3.2 and Palmer *et al.* [2003a]), we focus here on adjusting  $CH_4$  emissions only. Since the east Asian and Eurasian anthropogenic sources are two dominant components affecting the structure of  $CH_4$  Asian outflow during TRACE-P, we choose to fit the model to the observations by adjusting these two  $CH_4$  emission variables. We do not try to resolve the individual anthropogenic source components of  $CH_4$  within each region because of strong spatial source overlap (Figure 2), which precludes detection of individual signatures in the outflow.

[36] We focus on the data for Chinese outflow (Figure 6a), which provide the strongest regional constraints on sources and for which model transport errors are smallest because no vertical motions are involved [Kiley *et al.*, 2003]. The model with a priori sources overestimates the  $CH_4$  enhancement in this data set by 7 ppb (Figure 4b). The observed  $CH_4/C_2H_6$  and  $CH_4/CO$  slopes are  $43 \pm 1.2 \text{ mol mol}^{-1}$  and  $0.38 \pm 0.02 \text{ mol mol}^{-1}$ , respectively, while the corresponding model slopes are  $39 \pm 1.1 \text{ mol mol}^{-1}$  and  $0.38 \pm 0.02 \text{ mol mol}^{-1}$  (Table 3). We seek to satisfy the observed  $CH_4$  enhancements

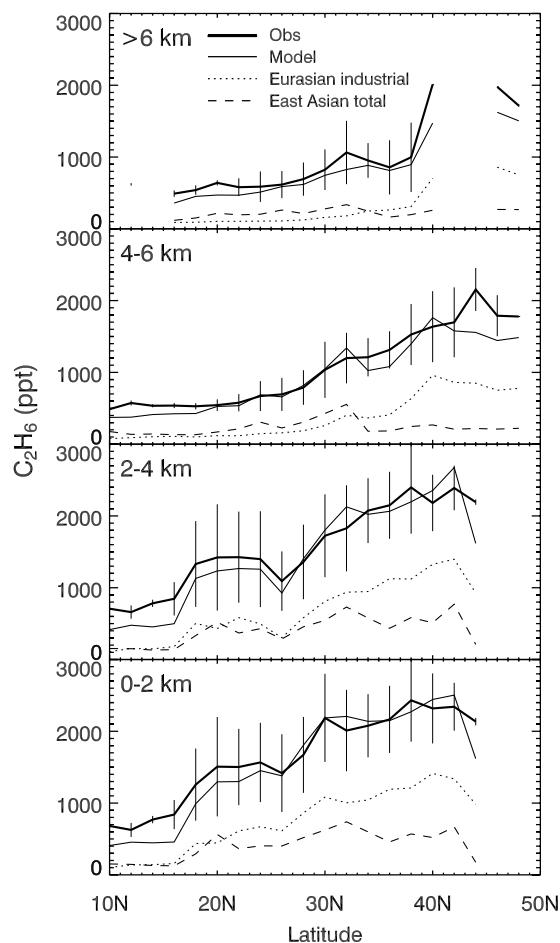


**Figure 5c.** Latitudinal dependence of  $C_2H_6$  concentrations along the TRACE-P flight tracks west of  $160^\circ E$  during TRACE-P at different altitudes. Observations (thick lines) are compared with model results (solid lines). The error bars represent standard deviations for the observations. Contributions of  $C_2H_6$  from east Asian (dashed) and Eurasian (dotted) tagged tracers in the model are also shown.

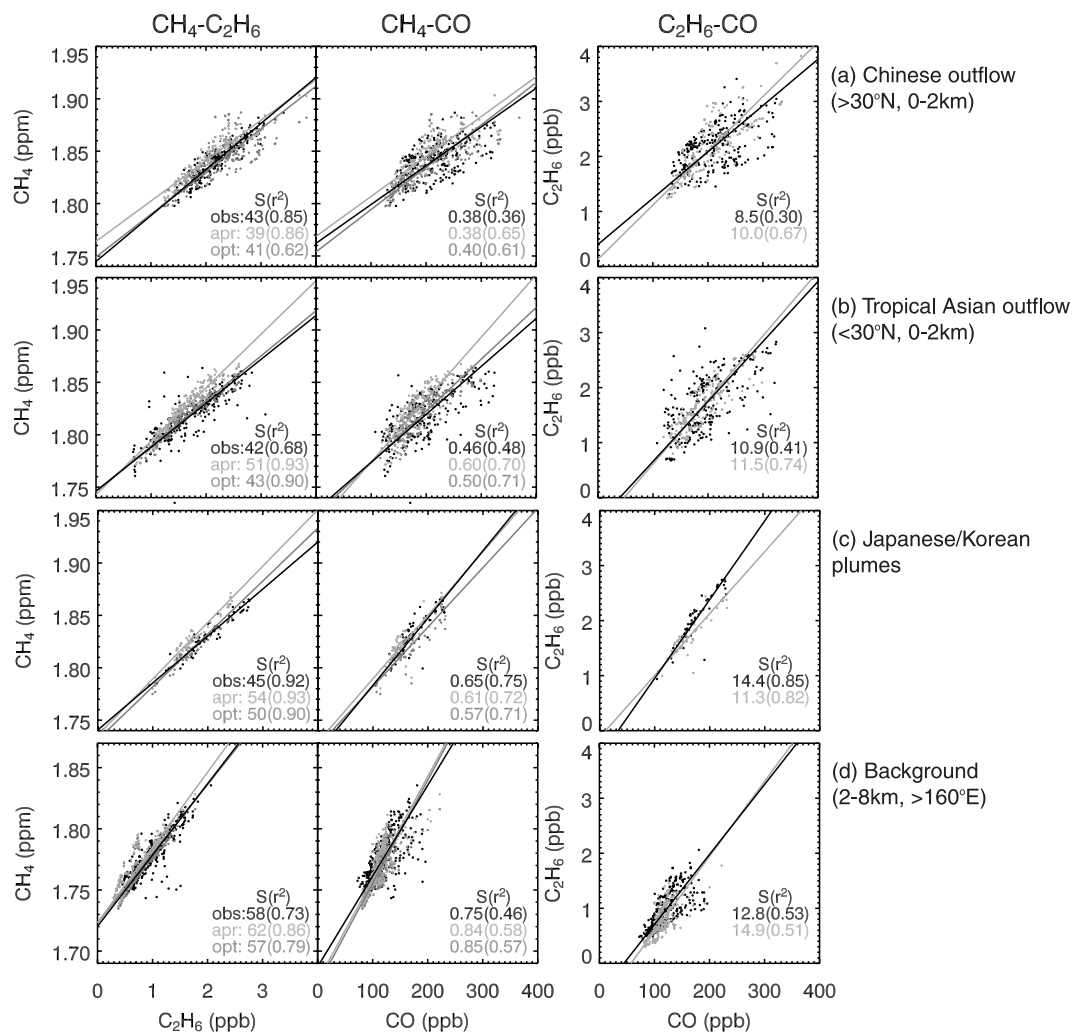


**Figure 6.** Simulated versus observed CH<sub>4</sub>-C<sub>2</sub>H<sub>6</sub>-CO correlations along the TRACE-P flight tracks in different regions. (a) Chinese outflow (>30°N and <2 km, west of 160°E), (b) tropical Asian outflow (<30°N and <2 km, west of 160°E), (c) Japanese/Korean plumes, and (d) background (2–8 km, east of 160°E). TRACE-P observations (“obs,” black) are compared with a priori model results (“apr,” green) and optimized model results (“opt,” red). The slopes (S) and r<sup>2</sup> of the RMA regression lines are shown (also in Table 3). See color version of this figure at back of this issue.

and the observed CH<sub>4</sub>/C<sub>2</sub>H<sub>6</sub> and CH<sub>4</sub>/CO correlations by adjusting CH<sub>4</sub> anthropogenic sources from east Asia and Eurasia in the model. Figure 7 shows the simulated CH<sub>4</sub>/C<sub>2</sub>H<sub>6</sub> and CH<sub>4</sub>/CO slopes and the difference between simulated and observed mean CH<sub>4</sub> concentration enhancements in the Chinese boundary layer outflow as a function of percentage changes in these two emission variables relative to the a priori. We aim to fit the observed mean CH<sub>4</sub> enhancements to within 5 ppb and the slopes to within the 95% confidence interval from the bootstrap method ( $\pm 1.96\sigma$ ), i.e., 40–46 for CH<sub>4</sub>/C<sub>2</sub>H<sub>6</sub> and 0.34–0.42 for CH<sub>4</sub>/CO. These ranges are shown as green and black lines in Figure 7. The domain of model space satisfying the three constraints is shaded in Figure 7. It defines our range of optimized east Asian and Eurasian anthropogenic emissions.

[37] The model simulation with a priori sources is represented by point A in Figure 7. The positive model bias in simulating the CH<sub>4</sub> concentration enhancement in Asian outflow could be caused by an overestimate of either east

Asian or Eurasian sources. We see from Figure 7 that simply decreasing either of these (or both) would cause the CH<sub>4</sub>/C<sub>2</sub>H<sub>6</sub> slope to be too low. Fitting the CH<sub>4</sub>/C<sub>2</sub>H<sub>6</sub> constraint requires an increase in east Asian emissions, and thus our solution involves increasing the east Asian and decreasing the Eurasian anthropogenic emissions both by at least 30% (point C).

[38] A 40% increase in springtime east Asian anthropogenic emissions relative to the a priori Wang *et al.* [2004] inventory can be achieved simply by using instead the emission inventory of Streets *et al.* [2003] (Table 1). Although that inventory is comparable to Wang *et al.* [2004] on an annual basis, it is 40% higher in March and April when the rice paddy source is at its seasonal minimum, as discussed in section 2. Such a 40% increase of east Asian sources requires from Figure 7 a corresponding decrease in Eurasian sources of 30–50%.

[39] Table 3 gives the simulated CH<sub>4</sub>/C<sub>2</sub>H<sub>6</sub> and CH<sub>4</sub>/CO slopes in the different TRACE-P regional data subsets for

**Table 3.** Slopes of CH<sub>4</sub>-C<sub>2</sub>H<sub>6</sub>-CO Relationships in Asian Outflow Over the NW Pacific (March to April 2001)<sup>a</sup>

		Chinese Outflow (>30°N, 0–2 km)	Tropical Asian Outflow (20–30°N, 0–2 km)	Japanese/Korean Outflow	Background (2–8 km, East of 160°E)
TRACE-P observations	CH <sub>4</sub> /C <sub>2</sub> H <sub>6</sub>	43 ± 1.2	42 ± 1.7	45 ± 1.6	58 ± 2.2
	CH <sub>4</sub> /CO	0.38 ± 0.02	0.46 ± 0.02	0.65 ± 0.03	0.75 ± 0.04
GEOS-CHEM: <sup>b</sup>	C <sub>2</sub> H <sub>6</sub> /CO	8.5 ± 0.5	10.9 ± 0.5	14.4 ± 0.6	12.8 ± 0.7
(1) A priori [ <i>Wang et al.</i> , 2004]	CH <sub>4</sub> /C <sub>2</sub> H <sub>6</sub>	39 ± 1.1	51 ± 0.9	54 ± 1.9	62 ± 1.3
	CH <sub>4</sub> /CO	0.38 ± 0.02	0.60 ± 0.02	0.61 ± 0.04	0.84 ± 0.05
	C <sub>2</sub> H <sub>6</sub> /CO	10.0 ± 0.4	11.5 ± 0.4	11.3 ± 0.6	14.9 ± 0.9
(2) A priori with <i>Streets et al.</i> [2003] anthropogenic East Asian emissions <sup>c</sup>	CH <sub>4</sub> /C <sub>2</sub> H <sub>6</sub>	47 ± 1.7	52 ± 1.2	59 ± 2.8	64 ± 1.2
	CH <sub>4</sub> /CO	0.45 ± 0.02	0.61 ± 0.03	0.67 ± 0.06	0.95 ± 0.05
(3) A priori with Eurasian sources reduced by 30–50% <sup>d</sup>	CH <sub>4</sub> /C <sub>2</sub> H <sub>6</sub>	33–35	44–47	45–49	55–57
	CH <sub>4</sub> /CO	0.32–0.34	0.50–0.54	0.51–0.55	0.82–0.86
(4) Optimized; cases 2 and 3 combined <sup>d</sup>	CH <sub>4</sub> /C <sub>2</sub> H <sub>6</sub>	41–43	43–46	50–54	57–59
	CH <sub>4</sub> /CO	0.40–0.41	0.50–0.54	0.57–0.61	0.85–0.88

<sup>a</sup>Slopes of the reduced-major-axis (RMA) regressions for the regional subsets of data shown in Figure 6, with standard deviations computed by the bootstrap method (see text). Units are mol/mol for CH<sub>4</sub>/C<sub>2</sub>H<sub>6</sub> and CH<sub>4</sub>/CO, 10<sup>-3</sup> mol/mol for C<sub>2</sub>H<sub>6</sub>/CO.

<sup>b</sup>Results shown for simulations with different CH<sub>4</sub> sources. For all scenarios the CO simulation is from *Palmer et al.* [2003a], in which Asian CO sources have been optimized through inversion analysis of the TRACE-P data, and C<sub>2</sub>H<sub>6</sub> sources are as described in section 2.2.2.

<sup>c</sup>Superseding the corresponding *Wang et al.* [2004] sources in east Asia (Table 1).

<sup>d</sup>Slopes are given as ranges, with the low and high ends corresponding to Eurasian anthropogenic emission reductions of 50% and 30%, respectively.

(1) the a priori simulation, (2) the a priori but with *Streets et al.* [2003] east Asian anthropogenic sources, (3) the a priori but with Eurasian anthropogenic sources decreased by 30–50%, and (4) the combination of cases 2 and 3. Using the *Streets et al.* [2003] emission inventory increases the CH<sub>4</sub>/C<sub>2</sub>H<sub>6</sub> and CH<sub>4</sub>/CO slopes in Chinese outflow, while decreasing the Eurasian sources decreases the slopes. Results with our optimized case 4 emissions indicate a general improvement in the simulation of the observed correlations for the tropical Asian as well as the Chinese boundary layer outflow, while there is little effect on the Japanese/Korean and background data subsets. The effects on the simulations of the CH<sub>4</sub> vertical profiles and the CH<sub>4</sub>-C<sub>2</sub>H<sub>6</sub>-CO correlations are shown in Figures 4a–4c and 6. The ability of the model to fit the observations is clearly improved; only the CH<sub>4</sub>/CO slopes in the Chinese outflow and Japanese/Korean outflow are slightly worse. With the optimized CH<sub>4</sub> sources, the simulated CH<sub>4</sub> concentrations in March 2001 at CMDL surface sites north of 30°N are 7 ppb lower on average than with the a priori simulation (Figure 3), while there is little difference south of 30°N.

[40] Our a priori total of 68 Tg yr<sup>-1</sup> for the Eurasian anthropogenic source from *Wang et al.* [2004] is comparable to that in the EDGAR3.2 [*Olivier and Berdowski*, 2001] bottom-up inventory (64 Tg yr<sup>-1</sup>). These inventories were constructed for the years 1998 and 1995, respectively. Aside from the intrinsic uncertainties in emission estimates, it is also likely that Eurasian emissions have decreased in recent years owing to increased mitigation efforts. Such mitigation efforts involve, for example, capture and utilization of CH<sub>4</sub> from landfills and coal mining and a shift from underground to surface mining of coal [*Olivier*, 2002a, 2002b; *Environmental Protection Agency (EPA)*, 2001]. Our results suggest that large decreases in Eurasian emissions of CH<sub>4</sub> could have taken place over the past decade.

## 5. Conclusions

[41] Large CH<sub>4</sub> enhancements above background were observed in Asian outflow over the NW Pacific during the TRACE-P aircraft mission (March and April, 2001). The

CH<sub>4</sub> enhancements showed strong correlations with C<sub>2</sub>H<sub>6</sub> and CO that varied with the outflow region. We used a global chemical transport model (GEOS-CHEM) simulation of the CH<sub>4</sub>-C<sub>2</sub>H<sub>6</sub>-CO system for the TRACE-P period to interpret these observations with the goal of better quantifying CH<sub>4</sub> regional sources.

[42] Our a priori model simulation uses the *Wang et al.* [2004] global CH<sub>4</sub> emission inventory previously derived from inverse modeling of NOAA/CMDL observations. It reproduces the general latitudinal and vertical distributions of CH<sub>4</sub> observed during TRACE-P but overestimates by about 7 ppb the CH<sub>4</sub> enhancement in Asian outflow. This enhancement is driven by anthropogenic sources in both east Asia and Eurasia (defined here as Europe and eastern Russia). The a priori model also underestimates the CH<sub>4</sub>/C<sub>2</sub>H<sub>6</sub> slopes in Chinese outflow and overestimates them in tropical Asian outflow and in Japanese/Korean plumes. It reproduces the observed CH<sub>4</sub>/CO slopes without significant bias except for an overestimate in tropical Asian outflow. We find that the CH<sub>4</sub>-C<sub>2</sub>H<sub>6</sub>-CO correlations in the Asian outflow observed in TRACE-P are defined mainly by anthropogenic sources of CH<sub>4</sub> (landfills, livestock, and fossil fuel) from east Asia and Eurasia, rather than by biomass burning or wetland sources from tropical Southeast Asia. Emissions from rice cultivation did not make a significant contribution to the CH<sub>4</sub> outflow in TRACE-P, in part because they are at low latitudes and in part because they were at their seasonal minimum during the TRACE-P period. Observations in late summer or early fall would be expected to see a stronger influence from rice cultivation CH<sub>4</sub> emissions.

[43] We employ the constraints offered by the observed CH<sub>4</sub> enhancements and the CH<sub>4</sub>-C<sub>2</sub>H<sub>6</sub>-CO correlations to optimize our estimates of the CH<sub>4</sub> anthropogenic emissions in east Asia and Eurasia. To correct the positive model bias of CH<sub>4</sub> concentrations in the boundary layer Chinese outflow while increasing the CH<sub>4</sub>/C<sub>2</sub>H<sub>6</sub> slope and maintaining the CH<sub>4</sub>/CO slope, we find that we need to increase the east Asian and decrease the Eurasian anthropogenic sources of CH<sub>4</sub> by at least 30% for both. The increase in east Asian emissions is imposed by the constraint on the CH<sub>4</sub>/C<sub>2</sub>H<sub>6</sub>

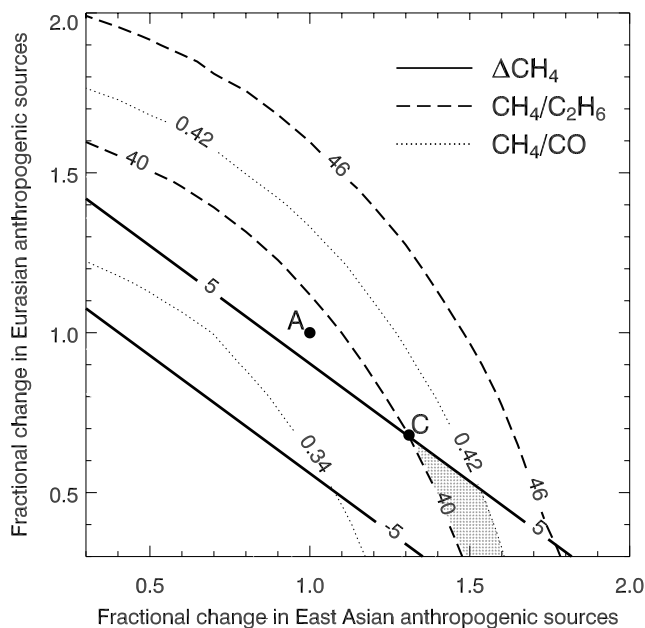


**Figure 7.** Constraints on east Asian and Eurasian  $\text{CH}_4$  sources from the  $\text{CH}_4$ - $\text{C}_2\text{H}_6$ - $\text{CO}$  correlations observed in Asian outflow during the TRACE-P aircraft mission. The figure shows GEOS-CHEM model results for the slopes ( $\text{mol mol}^{-1}$ ) of  $\text{CH}_4/\text{C}_2\text{H}_6$  (dashed lines) and  $\text{CH}_4/\text{CO}$  (dotted lines), and the difference in simulated and observed  $\text{CH}_4$  concentrations (solid lines), as a function of fractional changes of the east Asian and Eurasian anthropogenic sources of  $\text{CH}_4$  relative to the a priori. Values are shown for the Chinese boundary layer outflow (north of  $30^\circ\text{N}$  and below 2 km altitude). The shaded region defines the range of emissions compatible with the TRACE-P observations; we require the model to match the observed  $\text{CH}_4$  enhancement to within 5 ppb and the observed  $\text{CH}_4/\text{C}_2\text{H}_6$  and  $\text{CH}_4/\text{CO}$  slopes ( $43 \pm 3 \text{ mol mol}^{-1}$  and  $0.38 \pm 0.04 \text{ mol mol}^{-1}$ , respectively) to within 95% confidence intervals ( $\pm 1.96\sigma$ ). Point A (1, 1) represents the a priori emissions. Point C (1.3, 0.7) represents the minimum perturbation to the a priori emissions needed to fit the constraints from the TRACE-P observations: 30% increase and decrease of east Asian and Eurasian anthropogenic emissions, respectively.

slope. Without this increase, the model slope would be too low.

[44] A 40% increase in east Asian anthropogenic emissions for the TRACE-P period relative to the Wang *et al.* [2004] inventory can be implemented simply by substituting the Streets *et al.* [2003] regional inventory for east Asia prepared in support of the TRACE-P mission. The Streets *et al.* [2003] inventory has higher livestock and landfill emissions. The Eurasian anthropogenic source (80% European) then needs to be reduced by 30–50% from the Wang *et al.* [2004] inventory. Decrease of European  $\text{CH}_4$  emissions could have taken place over the past decade owing to mitigation efforts. Intrinsic uncertainties in the a priori emission inventory must also be considered.

[45] We have shown in this work that observed  $\text{CH}_4$ - $\text{C}_2\text{H}_6$ - $\text{CO}$  correlations in continental outflow place

valuable constraints on the  $\text{CH}_4$  budget. In our application these constraints allowed us to distinguish between east Asian and Eurasian source signatures in Asian outflow over the Pacific and to conclude that the overestimate of  $\text{CH}_4$  in our simulation with a priori sources had to be corrected by both decreasing the Eurasian source and (remarkably) increasing the east Asian source. A more formal inverse modeling approach for the  $\text{CH}_4$ - $\text{C}_2\text{H}_6$ - $\text{CO}$  system should be applied in a next stage to better exploit the constraints from the correlations. Improved understanding of  $\text{C}_2\text{H}_6$  sources (adjusted here in a top-down fashion to match observations) will be needed in order to better relate  $\text{CH}_4$ - $\text{C}_2\text{H}_6$  correlations to the fossil fuel source of  $\text{CH}_4$ .

[46] **Acknowledgments.** We thank Qinbin Li, Hongyu Liu, Mathew Evans, and John Lin for helpful discussions. This work was funded by the NASA Carbon Cycle Program and the NSF Atmospheric Chemistry Program.

## References

- Andreae, M. O., and P. Merlet (2001), Emission of trace gases and aerosols from biomass burning, *Global Biogeochem. Cycles*, *15*, 955–966.
- Bartlett, K. B., G. W. Sachse, J. E. Collins, and R. C. Harriss (1996), Methane in the tropical South Atlantic: Sources and distribution during the late dry season, *J. Geophys. Res.*, *101*, 24,139–24,150.
- Bartlett, K. B., G. W. Sachse, T. Slate, C. Harward, and D. B. Blake (2003), Large-scale distribution of  $\text{CH}_4$  in the western North Pacific: Sources and transport from the Asian continent, *J. Geophys. Res.*, *108*(D20), 8807, doi:10.1029/2002JD003076.
- Bertschi, I. T., R. J. Yokelson, D. E. Ward, T. J. Christian, and W. M. Hao (2003), Trace gas emissions from the production and use of domestic biofuels in Zambia measured by open-path Fourier transform infrared spectroscopy, *J. Geophys. Res.*, *108*(D13), 8469, doi:10.1029/2002JD002158.
- Bey, I., et al. (2001), Global modeling of tropospheric chemistry with assimilated meteorology: Model description and evaluation, *J. Geophys. Res.*, *106*, 23,073–23,096.
- Blake, D. R., and F. S. Rowland (1986), Global atmospheric concentrations and sources strength of ethane, *Nature*, *321*, 231–233.
- Blake, N. J., D. R. Blake, B. C. Sive, T.-Y. Chen, F. S. Rowland, J. E. Collins Jr., G. W. Sachse, and B. E. Anderson (1996), Biomass burning emissions and vertical distribution of atmospheric methyl halides and other reduced carbon gases in the South Atlantic region, *J. Geophys. Res.*, *101*, 24,151–25,164.
- Blake, N. J., et al. (2003), NMHCs and halocarbons in Asian continental outflow during TRACE-P: Comparison to PEM-West B, *J. Geophys. Res.*, *108*(D20), 8806, doi:10.1029/2002JD003367.
- Boissard, C., B. Bonsang, M. Kanakidou, and G. Lambert (1996), TROPOZ II: Global distributions and budgets of methane and light hydrocarbons, *J. Atmos. Chem.*, *25*, 115–148.
- Cicerone, R. J., and R. S. Oremland (1988), Biogeochemical aspects of atmospheric methane, *Global Biogeochem. Cycles*, *2*, 299–327.
- DeMore, W. B., et al. (1997), Chemical kinetics and photochemical data for use in stratospheric modeling, *JPL Publ. 97-4*, Jet Propul. Lab., Pasadena, Calif.
- Dlugokencky, E. J., L. P. Steele, P. M. Lang, and K. A. Masarie (1994), The growth rate and distribution of atmospheric methane, *J. Geophys. Res.*, *99*, 17,021–17,043.
- Dlugokencky, E. J., K. A. Masarie, P. M. Lang, and P. P. Tans (1998), Continuing decline in the growth rate of the atmospheric methane burden, *Nature*, *393*, 447–450.
- Dlugokencky, E. J., B. P. Walter, K. A. Masarie, P. M. Lang, and E. S. Kasischeke (2001), Measurements of an anomalous global methane increase during 1998, *Geophys. Res. Lett.*, *28*, 499–502.
- Duncan, B. N., R. V. Martin, A. C. Staudt, R. Yevich, and J. A. Logan (2003), Interannual and seasonal variability of biomass burning emissions constrained by satellite observations, *J. Geophys. Res.*, *108*(D2), 4100, doi:10.1029/2002JD002378.
- Environmental Protection Agency (EPA) (2001), Non- $\text{CO}_2$  greenhouse gas emissions from developed countries: 1990–2010, *Rep. EPA-430-R-01-007*, Washington, D. C.
- Etheridge, D. M., L. P. Steele, R. J. Francey, and R. L. Langenfelds (1998), Atmospheric methane between 1000 AD and present: Evidence of

- anthropogenic emissions and climatic variability, *J. Geophys. Res.*, *103*, 15,979–15,993.
- Fiore, A. M., D. J. Jacob, I. Bey, R. M. Yantosca, B. D. Field, and J. Wilkinson (2002), Background ozone over the United States in summer: Origin and contribution to pollution episodes, *J. Geophys. Res.*, *107*(D15), 4275, doi:10.1029/2001JD000982.
- Fiore, A. M., D. J. Jacob, H. Liu, R. M. Yantosca, T. D. Fairlie, and Q. Li (2003), Variability in surface ozone background over the United States: Implications for air quality policy, *J. Geophys. Res.*, *108*(D24), 4787, doi:10.1029/2003JD003855.
- Flores, R. M., J. H. Chen, V. G. Mcdonell, and G. S. Samuelsen (1999), Effect of natural gas composition on the performance of a model gas turbine combustor, combustion laboratory, paper presented at ATS Annual Workshop, Pittsburgh, Penn.
- Fuelberg, H. E., C. M. Kiley, J. R. Hannan, D. J. Westberg, M. A. Avery, and R. E. Newell (2003), Meteorological conditions and transport pathways during the Transport and Chemical Evolution over the Pacific (TRACE-P) experiment, *J. Geophys. Res.*, *108*(D20), 8782, doi:10.1029/2002JD003092.
- Fung, I., J. John, J. Lerner, E. Matthews, M. Prather, L. P. Steele, and P. J. Fraser (1991), Three-dimensional model synthesis of the global methane cycle, *J. Geophys. Res.*, *96*, 13,033–13,065.
- Gupta, M., S. Tyler, and R. Cicerone (1996), Modeling atmospheric  $\delta^{13}\text{C}_4$  and the causes of recent changes in atmospheric  $\text{CH}_4$  amounts, *J. Geophys. Res.*, *101*, 22,923–22,932.
- Gupta, M. L., R. J. Cicerone, D. R. Blake, F. S. Rowland, and I. S. A. Isaksen (1998), Global atmospheric distributions and source strengths of light hydrocarbons and tetrachloroethene, *J. Geophys. Res.*, *103*, 28,219–28,235.
- Hansen, J., M. Sato, R. Ruedy, A. Lacis, and V. Oinas (2000), Global warming in the twenty-first century: An alternative scenario, *Proc. Natl. Acad. Sci. USA*, *97*, 9875–9880.
- Harriss, R. C., G. W. Sachse, J. E. Collins Jr., L. Wade, K. B. Bartlett, R. W. Talbot, E. V. Browell, L. A. Barrie, G. F. Hill, and L. G. Burney (1994), Carbon monoxide and methane over Canada: July–August 1990, *J. Geophys. Res.*, *99*, 1659–1669.
- Heald, C. L., D. J. Jacob, P. I. Palmer, M. Evans, G. Sachse, D. Blake, and H. Singh (2003a), Biomass burning emission inventory with daily resolution: Application to aircraft observations of Asian outflow, *J. Geophys. Res.*, *108*(D21), 8811, doi:10.1029/2002JD003082.
- Heald, C. L., et al. (2003b), Asian outflow and trans-Pacific transport of carbon monoxide and ozone pollution: An integrated satellite, aircraft, and model perspective, *J. Geophys. Res.*, *108*(D24), 4804, doi:10.1029/2003JD003507.
- Hein, R., P. J. Crutzen, and M. Heimann (1997), An inverse modeling approach to investigate the global atmospheric methane cycle, *Global Biogeochem. Cycles*, *11*, 43–76.
- Hirsch, R. M., and E. J. Gilroy (1984), Methods of fitting a straight line to data: Examples in water resources, *Water Resour. Bull.*, *20*(5), 705–711.
- Houweling, S., T. Kaminski, F. Dentener, J. Lelieveld, and M. Heimann (1999), Inverse modeling of methane sources using the adjoint of a global transport model, *J. Geophys. Res.*, *104*, 16,160–26,137.
- Intergovernmental Panel on Climate Change (IPCC) (2001), Climate change 2001: The scientific basis, Geneva. (Available at [http://www.grida.no/climate/ipcc\\_tar/wgl1/index.htm](http://www.grida.no/climate/ipcc_tar/wgl1/index.htm))
- Jacob, D. J., J. H. Crawford, M. M. Kleb, V. S. Connors, R. J. Bendura, J. L. Raper, G. W. Sachse, J. C. Gille, L. Emmons, and C. L. Heald (2003), The Transport and Chemical Evolution over the Pacific (TRACE-P) aircraft mission: Design, execution, and first results, *J. Geophys. Res.*, *108*(D20), 9000, doi:10.1029/2002JD003276.
- Jaeglé, L., D. Jaffé, H. U. Price, P. Weiss, P. I. Palmer, M. J. Evans, D. J. Jacob, and I. Bey (2003), Sources and budgets for CO and O<sub>3</sub> in the northeastern Pacific during the spring of 2001: Results from the PHOBEA-II experiment, *J. Geophys. Res.*, *108*(D20), 8802, doi:10.1029/2002JD003121.
- Kanakidou, M., H. B. Singh, K. M. Valentin, and P. J. Crutzen (1991), A two-dimensional study of ethane and propane oxidation in the troposphere, *J. Geophys. Res.*, *96*, 15,395–15,413.
- Kiley, C. M., et al. (2003), An intercomparison and evaluation of aircraft-derived and simulated CO from seven chemical transport models during the TRACE-P experiment, *J. Geophys. Res.*, *108*(D21), 8819, doi:10.1029/2002JD003089.
- Lerner, J., E. Matthews, and I. Fung (1988), Methane emission from animals: A global high resolution data base, *Global Biogeochem. Cycles*, *2*, 139–156.
- Li, Q., D. J. Jacob, R. M. Yantosca, C. L. Heald, H. B. Singh, M. Koike, Y. Zhao, G. W. Sachse, and D. G. Streets (2003), A global 3-D model evaluation of the atmospheric budgets of HCN and CH<sub>3</sub>CN: Constraints from aircraft measurements over the western Pacific, *J. Geophys. Res.*, *108*(D21), 8827, doi:10.1029/2002JD003075.
- Liu, H., D. J. Jacob, I. Bey, R. M. Yantosca, B. N. Duncan, and G. W. Sachse (2003), Transport pathways for Asian combustion outflow over the Pacific: Interannual and seasonal variations, *J. Geophys. Res.*, *108*(D20), 8786, doi:10.1029/2002JD003102.
- Liu, H., D. J. Jacob, J. E. Dibb, A. M. Fiore, and R. M. Yantosca (2004), Constraints on the sources of tropospheric ozone from <sup>210</sup>Pb-<sup>7</sup>Be-O<sub>3</sub> correlations, *J. Geophys. Res.*, *109*, D07306, doi:10.1029/2003JD003988.
- Lowe, D. C., C. Brenninkmeijer, S. C. Tyler, and E. J. Dlugokencky (1991), Determination of the isotopic composition of atmospheric methane and its application in the Antarctic, *J. Geophys. Res.*, *96*, 15,455–15,467.
- Lowe, D. C., C. Brenninkmeijer, G. W. Brailsford, K. R. Lassey, A. J. Gomez, and E. G. Nisbet (1994), Concentration and C13 records of atmospheric methane in New Zealand and Antarctic: Evidence for changes in methane sources, *J. Geophys. Res.*, *99*, 16,913–16,925.
- Matsueda, H., and H. Y. Inoue (1999), Aircraft measurements of trace gases between Japan and Singapore in October of 1993, 1996, and 1997, *Geophys. Res. Lett.*, *26*, 2413–2416.
- Matthews, E., and I. Fung (1987), Methane emissions from natural wetlands: Global distribution, area, and ecology of sources, *Global Biogeochem. Cycles*, *1*, 61–86.
- Matthews, E., I. Fung, and J. Lerner (1991), Methane emissions from rice cultivation: Geographic and seasonal distribution of cultivated areas and emissions, *Global Biogeochem. Cycles*, *5*, 3–24.
- Miller, J. B., K. A. Mack, R. Dissly, J. W. C. White, E. J. Dlugokencky, and P. P. Tans (2002), Development of analytical methods and measurements of C-13/C-12 in atmospheric CH<sub>4</sub> from the NOAA Climate Monitoring and Diagnostics Laboratory global air sampling network, *J. Geophys. Res.*, *107*(D13), 4178, doi:10.1029/2001JD000630.
- Olivier, J. G. J. (2002a), Greenhouse gas emissions: 1. Shares and trends in greenhouse gas emissions, in *CO<sub>2</sub> Emissions From Fuel Combustion 1971–2000*, pp. 1–31, Int. Energy Agency (IEA), Paris.
- Olivier, J. G. J. (2002b), Greenhouse gas emissions: 2. Sources and methods, in *CO<sub>2</sub> Emissions From Fuel Combustion 1971–2000*, pp. 1–31, Int. Energy Agency (IEA), Paris.
- Olivier, J. G. J., and J. J. M. Berdowski (2001), Global emissions sources and sinks, in *The Climate System*, edited by J. Berdowski, R. Guicherit, and B. J. Heij, pp. 33–78, A.A. Balkema, Brookfield, Vt.
- Palmer, P. I., D. J. Jacob, D. B. Jones, C. L. Heald, R. M. Yantosca, J. A. Logan, G. W. Sachse, and D. G. Streets (2003a), Inverting for emissions of carbon monoxide from Asia using aircraft observations over the western Pacific, *J. Geophys. Res.*, *108*(D21), 8828, doi:10.1029/2003JD003397.
- Palmer, P. I., D. J. Jacob, L. J. Mickley, D. R. Blake, G. W. Sachse, H. E. Fuelberg, and C. M. Kiley (2003b), Eastern Asian emissions of anthropogenic halocarbons deduced from aircraft concentration data, *J. Geophys. Res.*, *108*(D24), 4753, doi:10.1029/2003JD003591.
- Prinn, R. G., R. F. Weiss, B. R. Miller, J. Huang, F. N. Alyea, D. M. Cunnold, P. J. Fraser, D. E. Hartley, and P. G. Simmonds (1995), Atmospheric trends and lifetime of CH<sub>2</sub>Cl<sub>2</sub> and global OH concentrations, *Science*, *269*, 187–192.
- Prinn, R. G., et al. (2001), Evidence for substantial variations of atmospheric hydroxyl radical in the past two decades, *Science*, *292*, 1882–1997.
- Quay, P., J. Stutsman, D. Wilbur, A. Snover, E. Dlugokencky, and T. Brown (1999), The isotopic composition of atmospheric methane, *Global Biogeochem. Cycles*, *13*, 445–461.
- Rudolph, J. (1995), The tropospheric distribution and budget of ethane, *J. Geophys. Res.*, *100*, 11,369–11,381.
- Russo, R. S., et al. (2003), Chemical composition of Asian continental outflow over the western Pacific: Results from Transport and Chemical Evolution over the Pacific (TRACE-P), *J. Geophys. Res.*, *108*(D20), 8804, doi:10.1029/2002JD003184.
- Shipham, M. C., P. M. Crill, K. B. Bartlett, A. H. Goldstein, P. M. Czepiel, R. C. Harriss, and D. Blaha (1998), Methane measurements in central New England: An assessment of regional transport from surrounding sources, *J. Geophys. Res.*, *103*, 21,985–22,000.
- Singh, H. B., A. Tabazadeh, M. J. Evans, B. D. Field, D. J. Jacob, G. W. Sachse, J. H. Crawford, R. Shetter, and W. H. Brune (2003), Oxygenated volatile organic chemicals in the oceans: Inferences and implications based on atmospheric observations and air-sea exchange models, *Geophys. Res. Lett.*, *30*(16), 1862, doi:10.1029/2003GL017933.
- Spivakovsky, C. M., et al. (2000), Three-dimensional climatological distribution of tropospheric OH: Update and evaluation, *J. Geophys. Res.*, *105*, 8931–8980.
- Staudt, A. C., D. J. Jacob, F. Ravetta, J. A. Logan, D. Bachiochi, T. N. Krishnamurti, S. Sandholm, B. Ridley, H. B. Singh, and B. Talbot (2003), Sources and chemistry of nitrogen oxides over the tropical Pacific, *J. Geophys. Res.*, *108*(D2), 8239, doi:10.1029/2002JD002139.

- Streets, D. G., et al. (2003), An inventory of gaseous and primary aerosol emissions in Asia in the year 2000, *J. Geophys. Res.*, *108*(D21), 8809, doi:10.1029/2002JD003093.
- Venables, W. N., and B. D. Ripley (1999), *Modern Applied Statistics with S-PLUS*, 3rd ed., Springer-Verlag, New York.
- Wang, Y. H., D. J. Jacob, and J. A. Logan (1998), Global simulation of tropospheric O<sub>3</sub>-NO<sub>x</sub>-hydrocarbon chemistry: 1. Model formulation, *J. Geophys. Res.*, *103*, 10,713–10,725.
- Wang, J. S., J. A. Logan, M. B. McElroy, B. N. Duncan, I. A. Megretskaya, and R. M. Yantosca (2004), A 3-D model analysis of the slowdown and interannual variability in the methane growth rate from 1988 to 1997, *Global Biogeochem. Cycles*, *19*, doi:10.1029/2003GB002180, in press.
- Yevich, R., and J. A. Logan (2003), An assessment of biofuel use and burning of agricultural waste in the developing world, *Global Biogeochem. Cycles*, *17*(4), 1095, doi:10.1029/2002GB001952.
- Yokelson, R. J., I. T. Bertschi, T. J. Christian, P. V. Hobbs, D. E. Ward, and W. M. Hao (2003), Trace gas measurements in nascent, aged, and cloud-processed smoke from African savanna fires by airborne Fourier transform infrared spectroscopy (AFTIR), *J. Geophys. Res.*, *108*(D13), 8478, doi:10.1029/2002JD002322.
- 
- D. R. Blake, Department of Chemistry, University of California, Irvine, CA 92697-2025, USA. (drblake@uci.edu)
- D. J. Jacob, J. A. Logan, P. I. Palmer, P. Suntharalingam, Y. Xiao, and R. M. Yantosca, Department of Earth and Planetary Sciences, Division of Engineering and Applied Sciences, Harvard University, Cambridge, MA 02138, USA. (djj@io.harvard.edu; jal@io.harvard.edu; pip@io.harvard.edu; pns@io.harvard.edu; xyp@io.harvard.edu; bmy@io.harvard.edu)
- G. W. Sachse, NASA Langley Research Center, Hampton, VA 23681, USA. (glen.w.sachse@nasa.gov)
- D. G. Streets, Argonne National Laboratory, Argonne, IL 60439, USA. (dstreets@anl.gov)
- J. S. Wang, Environmental Defense, New York, NY 10010, USA. (jwang@environmentaldefense.org)

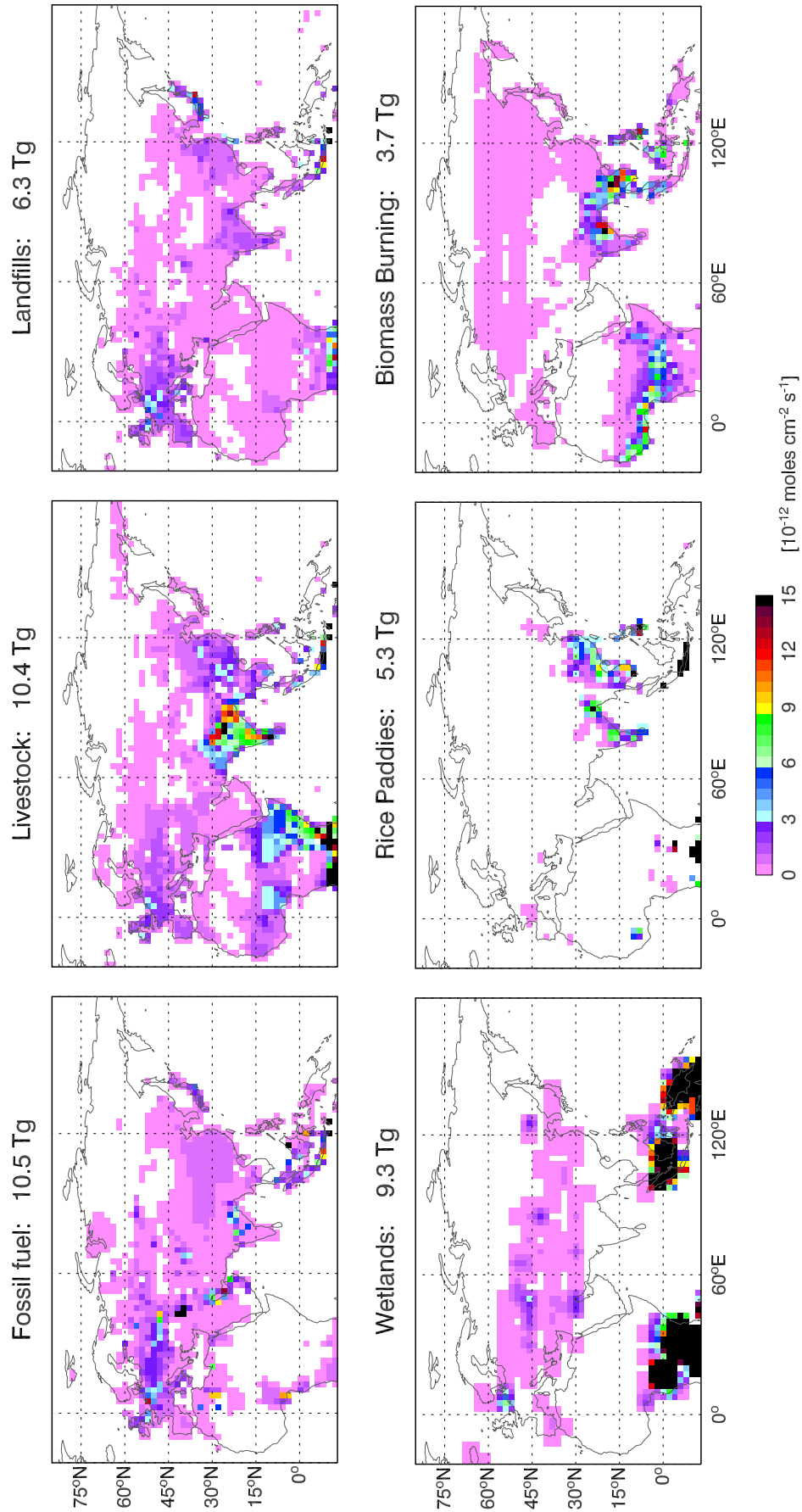


**Figure 2.** Distribution of CH<sub>4</sub> sources for the TRACE-P period (February to April, 2001) based on Wang *et al.* [2004] and used as a priori in this work. Total emissions from east Asian and Eurasian sources over the 3-month period are indicated for each source on the top of the corresponding panel.

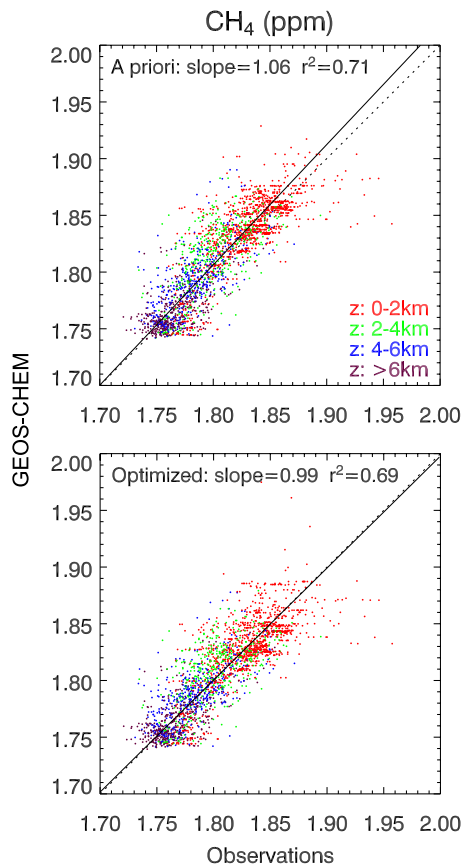


**Figure 4a.** Simulated versus observed concentrations of CH<sub>4</sub> along the TRACE-P flight tracks over the northwest Pacific (west of 160°E). Model results are shown for simulations with a priori (upper) and optimized (lower) emission inventories for CH<sub>4</sub>. The model is sampled along the flight tracks, and the observations are averaged over the model grid boxes. The 1:1 line is shown as dotted. The solid line is the reduced major axis (RMA) regression line. The a priori emission inventory is from Wang *et al.* [2004]. The optimized emission inventory uses east Asian anthropogenic emissions from Streets *et al.* [2003] and Eurasian anthropogenic emissions decreased by 50% from the Wang *et al.* [2004] inventory.

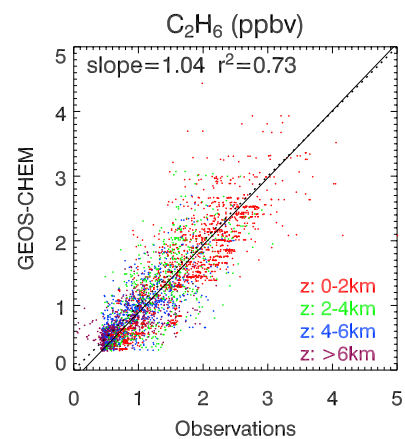


**Figure 5a.** Simulated versus observed concentrations of C<sub>2</sub>H<sub>6</sub> along the TRACE-P flight tracks over the northwest Pacific (west of 160°E). The observations are averaged over the model grid boxes. The 1:1 line is shown as dotted. The solid line is the RMA regression line.

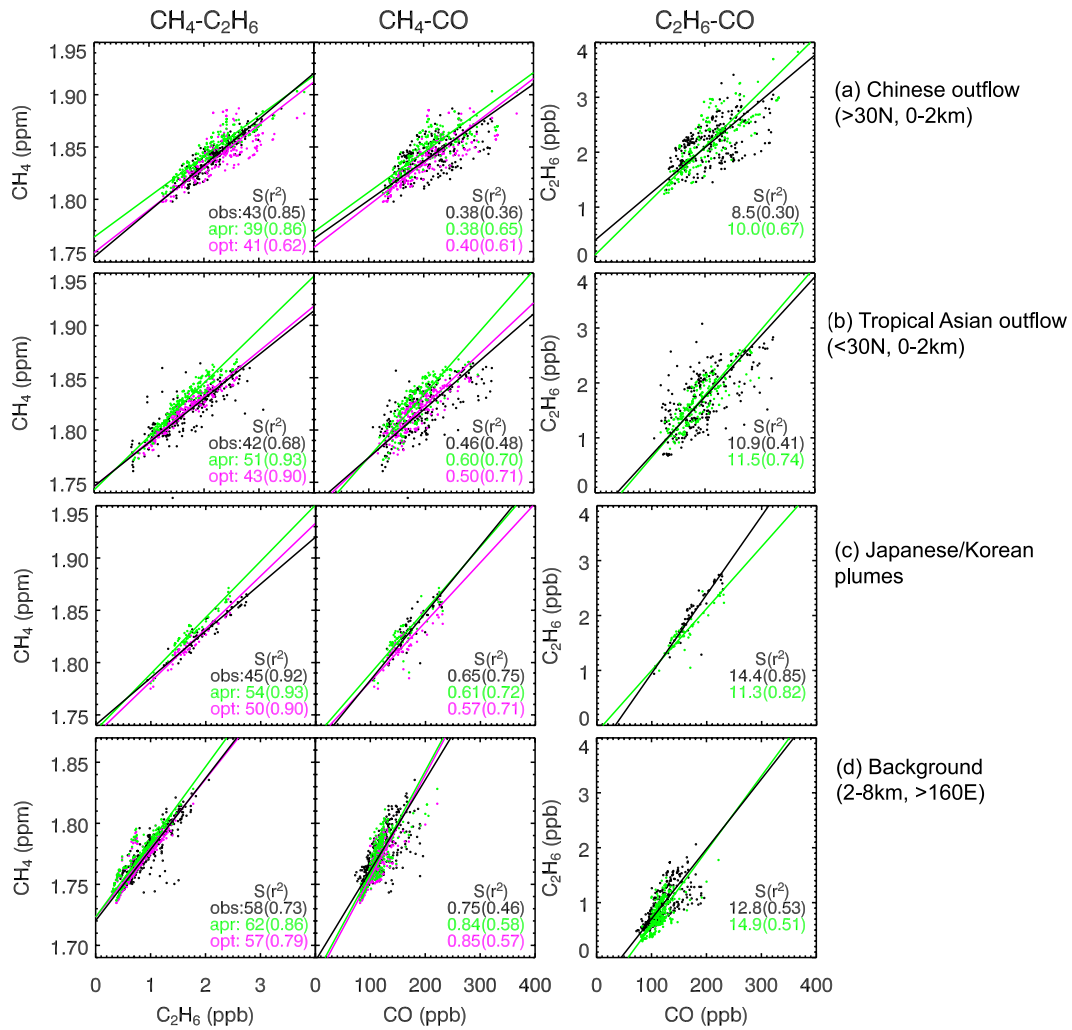


**Figure 6.** Simulated versus observed CH<sub>4</sub>-C<sub>2</sub>H<sub>6</sub>-CO correlations along the TRACE-P flight tracks in different regions. (a) Chinese outflow (>30°N and <2 km, west of 160°E), (b) tropical Asian outflow (<30°N and <2 km, west of 160°E), (c) Japanese/Korean plumes, and (d) background (2–8 km, east of 160°E). TRACE-P observations (“obs,” black) are compared with a priori model results (“apr,” green) and optimized model results (“opt,” red). The slopes (S) and r<sup>2</sup> of the RMA regression lines are shown (also in Table 3).